Accepted Manuscript

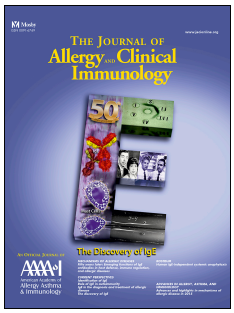

Novel Peptide Nanoparticle Biased Antagonist of CCR3 Blocks Eosinophil Recruitment and Airway Hyperresponsiveness

Milica Grozdanovic, PhD, Kimberly G. Laffey, PhD, Hazem Abdelkarim, PhD, Ben Hitchinson, BSc, Anantha Harijith, MD, Hyung-Geon Moon, PhD, Gye Young Park, MD, MSc, Lee K. Rousslang, BSc, Joanne C. Masterson, PhD, Glenn T. Furuta, MD, Nadya I. Tarasova, PhD, Vadim Gaponenko, PhD, Steven J. Ackerman, PhD

PII: S0091-6749(18)30709-7

DOI: 10.1016/j.jaci.2018.05.003

Reference: YMAI 13430

To appear in: *Journal of Allergy and Clinical Immunology*

Received Date: 8 December 2017

Revised Date: 7 May 2018

Accepted Date: 11 May 2018

Please cite this article as: Grozdanovic M, Laffey KG, Abdelkarim H, Hitchinson B, Harijith A, Moon H-G, Park GY, Rousslang LK, Masterson JC, Furuta GT, Tarasova NI, Gaponenko V, Ackerman SJ, Novel Peptide Nanoparticle Biased Antagonist of CCR3 Blocks Eosinophil Recruitment and Airway Hyperresponsiveness, *Journal of Allergy and Clinical Immunology* (2018), doi: 10.1016/j.jaci.2018.05.003.

R321 Biased Antagonism of CCR3 Inhibits Eosinophil Recruitment and Blocks Airway Hyperresponsiveness

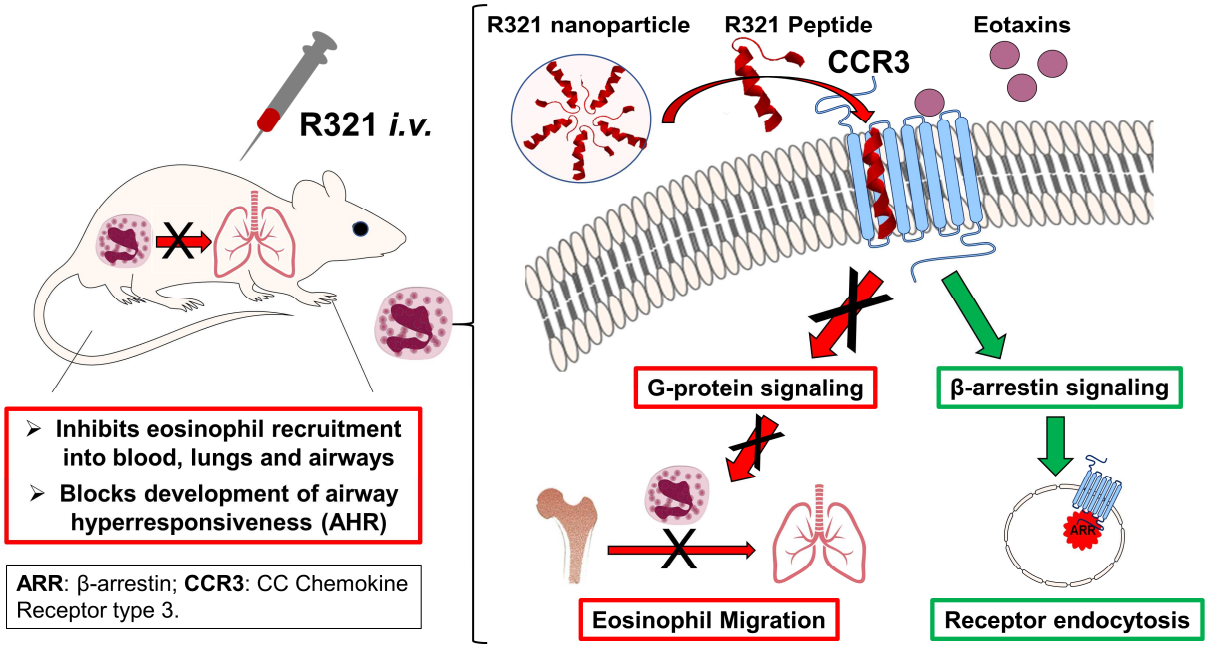

- Inhibits eosinophil recruitment into blood, lungs and airways
- Blocks development of airway hyperresponsiveness (AHR)

ARR: β-arrestin; **CCR3**: CC Chemokine Receptor type 3.

Novel Peptide Nanoparticle Biased Antagonist of CCR3 Blocks Eosinophil Recruitment and Airway Hyperresponsiveness

Milica Grozdanovic, PhD,[1, 2] Kimberly G. Laffey, PhD,[1, 2] Hazem Abdelkarim, PhD,[1] Ben Hitchinson, BSc,[1] Anantha Harijith, MD,[3] Hyung-Geon Moon, PhD,[4] Gye Young Park, MD, MSc,[4] Lee K. Rousslang, BSc,[1] Joanne C. Masterson, PhD,[5] Glenn T. Furuta, MD,[5] Nadya I. Tarasova, PhD,[6] Vadim Gaponenko, PhD,[1,7] and Steven J. Ackerman, PhD[1,7]

[1]Department of Biochemistry and Molecular Genetics, College of Medicine, University of Illinois at Chicago, Chicago IL

[2]These co-first authors contributed equally to this work

[3]Department of Pediatrics, College of medicine, University of Illinois at Chicago, Chicago, IL

[4]Department of Medicine, Division of Pulmonary, Critical Care, Sleep & Allergy, College of Medicine, University of Illinois at Chicago, Chicago IL

[5]Gastrointestinal Eosinophilic Diseases Program, Department of Pediatrics, University of Colorado School of Medicine; Digestive Health Institute, Children's Hospital Colorado, Mucosal Inflammation Program, University of Colorado School of Medicine, Aurora, CO.

[6]Center for Cancer Research, National Cancer Institute, Frederick, MD.

[7]These co-senior authors contributed equally to this work

Corresponding Authors: Steven J. Ackerman, PhD and Vadim Gaponenko, PhD

Address for correspondence: Steven J. Ackerman, PhD. Department of Biochemistry and Molecular Genetics, College of Medicine, University of Illinois at Chicago, MBRB 2074, MC669, 900 S. Ashland Ave, Chicago, IL 60607

Telephone: (312) 996-6149

Fax: (312) 996-5623

E-mail: sackerma@uic.edu

Funding Sources: This work was supported in part by NIH Grants R21HL118588 (SJA/VG), R01HL126852 (GYP), K01DK106315 (JCM), K24DK100303 (GTF), the LaCache Chair for GI Allergic and Immunologic Diseases (GTF), and a grant from the University of Illinois at Chicago Chancellors Innovation Fund – Proof of Concept program (SJA/VG), and the Intramural Research Program of the National Cancer Institute, NIH (NIT). HA was supported in part by a postdoctoral fellowship from the American Parkinson Disease Association (APDA). The content is solely the responsibility of the authors and does not necessarily represent the official views of the NIH. These funding sources had no involvement in study design; in the collection, analysis and interpretation of data; in the writing of the report; and in the decision to submit the article for publication.

Statement of Possible Conflicts of Interest: MG, no conflicts to disclose; KGL, co-inventor of the CCR3 R321 peptide-see below, no other conflicts to disclose; HA, co-inventor of the CCR3 R321 peptide-see below, supported by a postdoctoral fellowship from the American Parkinson Disease Association; BH, co-inventor of the CCR3 R321 peptide-see below; AH, no conflicts to disclose; H-GM, no conflicts to disclose; GYP,

supported by NIH grant R01HL126852, no conflicts to disclose; LKR, no conflicts to disclose; JCM, supported by NIH grant K01DK106315, no conflicts to disclose; GTF, supported by NIH grant K24DK100303, LaCache Chair for GI Allergic and Immunologic Diseases, is a co-founder of EnteroTrack, LLC, receives royalties from UpToDate and serves as consultant for Shire; NIT, co-inventor of the CCR3 R321 peptide-see below, supported by the Intramural Research Program of the National Cancer Institute; VG, co-inventor of the CCR3 R321 peptide-see below, supported by NIH Grant R21HL118588 and a grant from the University of Illinois at Chicago Chancellors Innovation Fund–Proof of Concept program; SJA, co-inventor of the CCR3 R321 peptide-see below, supported by NIH Grant R21HL118588 and a grant from the University of Illinois at Chicago Chancellors Innovation Fund – Proof of Concept program, co-founder/co-owner, Chief Scientific Officer and consultant for EnteroTrack, LLC. The IP for the CCR3 R321 peptide nanoparticle biased antagonist was submitted as a US patent entitled “Peptide inhibition of CCR3-mediated diseases and conditions” on Feb. 12, 2016 (PCT/US2016/017714). Co-authors KGL, HA, BH, NIT, VG and SJA are co-inventors; the IP is jointly owned by UIC and NIH/NCI. The PCT application was nationalized (European Patent Office EP16749945.8) on Aug. 12, 2017, and is being filed in Canada.

Key Messages:

- R321 is a novel biased nanoparticle CCR3 antagonist that inhibits G-protein signaling but not β-arrestin-mediated CCR3 internalization and degradation
- R321 blocks eosinophil recruitment into the blood, lungs and airways and prevents airway hyperresponsiveness in a mouse eosinophilic asthma model

Capsule summary: Chemokine receptor CCR3 is a promising target for blocking eosinophil recruitment in allergic diseases. We developed a novel CCR3 antagonist that blocks eosinophil migration, prevents development of airway hyperresponsiveness, and avoids the development of tolerance.

Key Words: CCR3, eosinophil, allergic inflammation, asthma, biased antagonist, peptide nanoparticles, airway hyperresponsiveness

Short Running Title: Biased antagonism of CCR3-mediated eosinophil function

Abbreviations: AHR, Airway Hyperresponsiveness; BALF, Bronchoalveolar lavage fluid; CCR3, C-C chemokine receptor 3; DRA, Dust mite, Ragweed, and *Aspergillus*; DLS, dynamic light scattering; ECP, eosinophil cationic protein; EoE, Eosinophilic Esophagitis; GPCR, G-protein-coupled receptor; NMR, Nuclear Magnetic Resonance; PAF, platelet-activating factor.

ABSTRACT

Background: Chemokine signaling through CCR3 is a key regulatory pathway for eosinophil recruitment into tissues associated with allergic inflammation and asthma. To date, none of the CCR3 antagonists have shown efficacy in clinical trials. One reason may be their unbiased mode of inhibition that prevents receptor internalization, leading to drug tolerance.

Objective: We sought to develop a novel peptide nanoparticle CCR3 inhibitor (R321) with a biased mode of inhibition that would block G-protein signaling, but enable or promote receptor internalization.

Methods: Self-assembly of R321 peptide into nanoparticles and peptide binding to CCR3 were analyzed by dynamic light scattering and NMR. Inhibitory activity on CCR3 signaling was assessed *in vitro* using flow cytometry, confocal microscopy, and western blot analysis in a CCR3+ eosinophil cell line and blood eosinophils. *In vivo* effects of R321 were assessed using a triple allergen mouse asthma model.

Results: R321 self-assembles into nanoparticles and binds directly to CCR3, altering receptor function. IC_{50} values for eotaxin-induced chemotaxis of blood eosinophils are in the low nanomolar range. R321 inhibits only the early phase of ERK1/2 activation and not the late phase generally associated with β-arrestin recruitment and receptor endocytosis, promoting CCR3 internalization and degradation. *In vivo*, R321 effectively blocks eosinophil recruitment into the lungs and airways and prevents airway hyperresponsiveness in a mouse eosinophilic asthma model.

Conclusions: R321 is a potent and selective antagonist of the CCR3 signaling cascade. Inhibition through a biased mode of antagonism may hold significant therapeutic promise by eluding the formation of drug tolerance.

INTRODUCTION

In allergic disorders, such as asthma and eosinophilic esophagitis (EoE), eosinophils are recruited into the lung and esophagus, respectively, and activated in excess at these sites of inflammation. In these diseases, eosinophils are both a histologic hallmark and among the major effector cell types contributing to their pathology[1, 2]. The C-C chemokine receptor 3 (CCR3) signaling pathway is one of the key regulatory pathways involved in eosinophil recruitment and migration into the affected tissues as part of the allergic diathesis.

While CCR3 is most highly expressed by eosinophils, it is also expressed by basophils, subsets of mast cells and Th2 cells, and airway epithelial cells[3-5]. CCR3 is a promiscuous G-protein-coupled receptor (GPCR), interacting with multiple inflammatory chemokines, including the high affinity agonists eotaxin-1 (CCL11), eotaxin-2 (CCL24), eotaxin-3 (CCL26), and RANTES (CCL5). The receptor is coupled to the pertussis toxin-sensitive G protein Gαi. Upon ligand binding, the receptor is activated and active GTP-bound Gαi and the Gβγ dimer dissociate from CCR3 to trigger downstream signaling cascades including the MAPK (ERK1/2, p38) and the PI3K/AKT pathways[6, 7]. These intracellular signaling pathways culminate in priming, chemotaxis, activation, and degranulation of eosinophils. Following receptor activation by the ligand, CCR3 is desensitized and internalized[8, 9]. The mechanism of CCR3 internalization is not yet fully understood, but is thought to occur via β-arrestin recruitment to phosphorylated CCR3

and sequestration of the receptor into endosomes[10]. In addition, eotaxin-induced CCR3 internalization may be required for actin polymerization and chemotaxis[9].

The importance of CCR3 as a potential therapeutic target was established through the observations that CCR3-null mice and eotaxin-1 and eotaxin-2 double knockout mice displayed near complete abolishment (up to ~70%) of allergen-induced airway eosinophil recruitment[11]. CCR3 transcript and protein levels are increased in the bronchial mucosa of patients with allergic asthma[12]. In line with this, much effort has been invested in the development of small molecule CCR3 antagonists, yet none have been approved for clinical use to date[4].

Most of the currently known CCR3 antagonists are competitive or allosteric inhibitors of CCR3 activation and internalization by chemokines[4]. The dual inhibitory activity of these molecules classifies them as *unbiased antagonists*. Reports on the use of unbiased antagonists of other GPCRs, such as CXCR4, suggest that after prolonged exposure, cell surface GPCR accumulates, a phenomenon associated with developing resistance to receptor inhibition[13, 14]. These findings prompted us to search for antagonists that can "bias" downstream signaling by selectively inhibiting only one of the signaling cascades. There is a growing interest in the development of *biased agonists* of GPCRs,[15] but *biased antagonists* of GPCRs remain largely unexplored, very few have been identified, and their therapeutic potential remains to be determined.

In the present study, we report the development and validation of R321, a novel peptide inhibitor derived from the second transmembrane helix of CCR3. R321 self-assembles into uniform nanoparticles and inhibits CCR3-mediated chemotaxis of human blood eosinophils with nanomolar potencies. Intravenously administered R321 significantly reduces eosinophil recruitment into the lung and airspaces and diminishes airway hyperresponsiveness (AHR) in a triple allergen (DRA) mouse asthma model of allergic airway inflammation. We propose that the R321 peptide exerts its receptor inhibitory effects on eosinophil function as a *biased antagonist* by inhibiting G-protein mediated processes and promoting the internalization (endocytosis) and degradation of CCR3.

MATERIALS AND METHODS

Reagents

Small molecule CCR3 antagonists, SB238437 and UCB35625, were purchased from Tocris Bioscience (Bristol, UK).

Peptide synthesis and characterization

Synthesis, purification and evaluation of nanoparticle formation of R321 and R323 peptides were performed as described in the Supplementary Materials.

Cell culture

AML14.3D10-CCR3 cells, an eosinophil-differentiated acute myeloid leukemia cell line stably transfected to express CCR3 (ATCC® CRL-12079), were cultured as previously described.[16] Jurkat cells, a T cell leukemia line endogenously expressing CXCR4, but not CCR3, were cultured in RPMI-1640 supplemented with 10% FBS, 1% Penicillin-streptomycin, and 2 mM L-Glutamine.

Eosinophil purification

Eosinophils were purified from blood drawn from mild allergic asthmatic subjects. Peripheral blood was separated over a gradient of Ficoll-Paque Plus (GE Healthcare, Pittsburg, PA). Eosinophils were further purified by negative selection using a commercial Eosinophil Isolation kit (MAC Miltenyi Biotec, Auburn, CA).

Chemotaxis and degranulation assays

Chemotaxis and degranulation assays are described in the Supplementary Materials.

Prolonged exposure to inhibitors

AML14.3D10-CCR3 cells or human peripheral blood eosinophils were incubated for 24, 48, or 72 hours with either vehicle control or 1 µM inhibitors. Cells were resuspended in fresh complete medium with inhibitors every day.

Signal transduction – western blotting and confocal microscopy

Detailed descriptions are provided in the Supplementary Materials.

Receptor expression and internalization

To evaluate CCR3 cell surface expression and ligand-induced internalization, cells were treated for 30 min with vehicle control, R321 (0.01-10 µM) ± CCL11 (12 nM), or R323, SB238437, UCB35625 (all at 1µM) ± CCL11 (12nM). Cells were blocked with 10% heat-inactivated human AB-serum, stained using PE-conjugated anti-human CCR3 antibody (clone 5E8, BioLegend, San Diego, CA) or PE-conjugated isotype-matched control (BioLegend, San Diego, CA) and analyzed on a Quanta SC flow cytometer (Beckman Coulter, Indianapolis, IN). Cell surface staining and gating strategy employed for the enumeration of mouse blood eosinophils and determination of CCR3 surface expression levels is described in the Supplementary Materials.

Mice

Female BALB/cJ mice (10-12 weeks of age) were purchased from The Jackson Laboratory (Bar Harbor, ME). All animal study protocols were reviewed and approved by the Institutional Animal Care and Use Committee of the University of Illinois (Chicago, IL).

Sensitization and airway challenge

Sensitization and intranasal challenges were performed according to the acute asthma protocol previously described by Goplen at al[17]. In brief, mice were sensitized twice *ip* with a cocktail of 3 allergens: Dust-mite (*D. Farinae*) – 5 µg, ragweed (*A. artemisifolia*) – 50 µg, and *Aspergillus fumigatus* – 5 µg. All extracts were purchased from Greer Laboratories (Lenoir, NC). One week after the second sensitization, intranasal challenges consisting of 0.15 µg of *Aspergillus*, 0.15 µg of dust-mite, and 1.5 µg of ragweed extract were given for 3 consecutive days. Control mice were sham-challenged with PBS. For the prophylactic protocol, R321, scrambled R323 peptide control, vehicle, or PBS was delivered by *iv* injection into the retro-orbital sinus one day before the first challenge and directly prior to each subsequent challenge. For the therapeutic protocol, mice started receiving 12 mg/kg of R321 or R323 on the day after the final allergen challenge and for 3 additional days following the date of the last challenge.

Bronchoalveolar lavage, lung histology and airway responsiveness to methacholine

Bronchoalveolar lavage (BAL) was performed as described in the Supplementary Materials. Whole lungs were fixed in 10% formalin and embedded in paraffin. Lung

tissue sections were stained with rat anti-mouse MBP1 antibody (generously provided by the Lee laboratories, Mayo Clinic, Scottsdale, AZ) as previously described.[18] Immunostained slides were scanned using Aperio Scanscope CS2 scanner (Aperio, Vista, CA) and analyzed with Aperio's image viewer software. Nuclei were counterstained with Mayer's Hematoxylin and cell counts were expressed as percent of MBP1 positive cells of the total nucleated cell count. Determination of airway responsiveness to methacholine is described in the Supplementary materials.

NMR

NMR was performed as described in the Supplementary Materials.

Statistical Analysis

Statistical analysis was performed using two-tailed t-tests, one way or two-way ANOVA, followed by Tukey *post hoc* analysis in GraphPad Prism software (GraphPad, San Diego, CA).

RESULTS

R321 self-assembles into nanoparticles

Peptides containing sequences from each of the seven transmembrane domains and associated extracellular loops of human CCR3 were first screened for inhibition of chemotaxis to CCL11, identifying the second transmembrane domain and first extracellular loop region as the most inhibitory (data not shown). The final design of R321 (**Fig. 1A**) was based on a previously described self-assembling CXCR4 peptide antagonist[19, 20]. Twenty-seven units of polyethylene glycol (PEG) were placed on the C-terminus of the peptide to prevent aggregation, and the PEG units were followed by three aspartate residues that ensure homogeneous self-assembly and correct orientation upon membrane fusion (**Fig. 1A**). The control peptide, R323, was derived by randomly, but separately, scrambling the sequences of the R321 transmembrane and extracellular loop regions (**Fig. 1A**). DLS analysis (**Fig. 1B**) showed that R321 and R323 monomers both self-assemble in an aqueous environment into nanospheres with a hydrodynamic radius of 7.1± 0.7 nm and 4.5 ± 0.4 nm, respectively, with R323 smaller and more polydisperse than R321. The size of the R321 particles was maintained over a wide range of monomeric concentrations (**Fig. 1C**).

R321 specifically inhibits eotaxin-induced eosinophil chemotaxis

Human blood eosinophils and the stable CCR3+ eosinophilic myelocyte cell line, AML14.3D10-CCR3, undergo CCR3-mediated chemotaxis induced by multiple chemokines including CCL11/eotaxin-1, CCL24/eotaxin-2, and CCL26/eotaxin-3 (**Fig.**

2). R321 was observed to inhibit eotaxin-induced chemotaxis by both primary eosinophils (**Fig. 2A**) and the AML14.3D10-CCR3 cell line (**Fig. 2B**) in a dose-dependent manner and with nanomolar potencies. The IC_{50} and IC_{90} values are shown in **Fig. 2C**. When used at a concentration of 1 µM (approximate IC_{90} value for R321), the scrambled peptide control (R323) failed to significantly inhibit eotaxin-mediated chemotaxis in blood eosinophils (**Fig. 2D**). R321 failed to inhibit CXCR4-mediated chemotaxis in Jurkat T-cells (**Fig. 2E**) and platelet-activating factor (PAF)-mediated chemotaxis of blood eosinophils (**Supplementary Fig. S1**), demonstrating the specificity of R321 inhibition of CCR3. Although CCR3 ligands induce degranulation of cytochalasin-B treated human eosinophils,[21] R321 did not promote CCL11-induced degranulation and secretion of eosinophil cationic protein (ECP) in blood eosinophils (**Supplementary Fig. S2**).

Effects of R321 on CCR3 signal transduction pathways

R321 was found to inhibit the activation of Gαi in an immunoprecipitation assay that detects Gαi-GTP (**Fig. 3A**) but did not inhibit receptor degradation (**Fig. 3B**). Pretreatment of AML14.3D10-CCR3 cells with 10 µM R321 (a concentration exceeding IC_{50} and IC_{90} for chemotaxis) before exposure to ligands was even found to enhance degradation of the CCR3 receptor (**Fig. 3B**). Both G-protein and β-arrestin mediated signaling pathways can lead to AKT and ERK 1/2 activation, although the time course of activation through the two pathways is different, leading to biphasic phosphorylation.[22-25] Following stimulation of AML14.3D10-CCR3 cells with chemokines, biphasic phosphorylation of AKT (**Fig. 3C**) and ERK 1/2 (**Fig. 4A**) was observed in western blots.

The early (2-5min) phosphorylation is mediated by G-protein signaling. The late sustained phase (30 min) phosphorylation is likely due to β-arrestin signaling as demonstrated for other GPCRs.[22, 25, 26] Pretreatment of cells for 30 min with 10 μM R321 prior to stimulation lead to a complete inhibition of the early phase of ERK 1/2 activation (5 min) but had no effect on the prolonged late phase (30 min). The control peptide, R323, had no effect on ERK1/2 phosphorylation patterns. Both SB328437 and UCB35625 fully inhibited the late phase, with SB328437 blocking the early phase as well, and UCB35625 doing so only partially (**Fig. 4A**). These results indicate that, unlike SB328437 and UCB35625, R321 does not inhibit the β-arrestin signaling that mediates the late phase phosphorylation of ERK1/2.

R321 does not antagonize β-arrestin recruitment to CCR3

Co-localization of CCR3 and β-arrestin 2 was observed following stimulation of CCR3 with CCL11 (**Fig. 4B**), suggesting that β-arrestin plays a role in ligand-induced CCR3 internalization and degradation. Pretreatment of cells with 10 μM R321 or R323 did not significantly ($p>0.05$) alter the reported co-localization coefficients either before or after CCL11 stimulation (**Fig. 4C**). In contrast, co-localization of CCR3 and β-arrestin 2 was significantly attenuated after treatment with UCB35625 and SB328437 when compared to untreated cells ($p\leq0.0001$) (**Fig. 4C**). Representative images of antibody controls can be found in **Supplementary Fig. S3**.

R321 promotes rather than inhibits CCR3 internalization and degradation

Inhibition of β-arrestin signaling may interfere with effective degradation of CCR3 and lead to receptor accumulation on the eosinophil cell surface. To elucidate the fate of CCR3 upon ligand and inhibitor treatment, surface levels of CCR3 in AML14.3D10-CCR3 cells were determined by flow cytometry. More than 50% of CCR3 present on the cell surface was internalized following 30 min of CCL11 exposure, in keeping with previous reports[8, 27]. R321 and the scrambled R321 peptide control showed no significant effect on ligand-induced receptor internalization, whereas the small molecule antagonists, UCB35625 and SB328437, partially blocked CCR3 internalization and degradation (**Fig. 5A**). Of note, R321 at 10 µM was found to promote CCR3 internalization on its own, without the addition of chemokine ligand (**Fig. 5B**).

R321 maintains its efficacy over 72h in contrast to unbiased antagonists

The effects of prolonged exposure to inhibitors on CCL11-induced chemotaxis and CCR3 surface expression was assessed for up to 72h in AML14.3D10-CCR3 cells and in blood eosinophils (**Fig. 5C and 5D**). CCL11 (12 nM) alone and CCL11 + R321 reduced CCR3 expression to ~68% and ~55%, respectively, after 24h, and to ~18% and ~12% after 72h (**Fig. 5D**). Treatment of cells for 72h with R321 alone reduced surface levels of CCR3 to 68%, as compared to untreated cells. In contrast, UCB35625 lead to receptor accumulation on the surface and enhanced CCR3 surface levels up to 133% after 72h. R323 and SB328437 had no significant effect on receptor levels. A similar effect was observed on CCR3 surface expression in AML14.3D10-CCR3 cells (**Supplementary Fig. S4**). In agreement with the levels of CCR3 expression detected, R321 did not lose any of its inhibitory potency during 72h of treatment (maintaining 90%

inhibition of chemotaxis), while UCB35625 and SB328437 inhibition levels dropped by 19.3% and 13.7%, respectively (**Fig. 5C**). These results indicate that resistance to the small molecule inhibitors, but not to R321, develops over time.

R321 inhibits eosinophil recruitment into the lung and airspaces

In a robust mouse DRA allergic asthma model of eosinophilic airway inflammation (**Fig. 6A**), prophylactically (**Supplementary Fig. S5A**) administered *iv* R321 demonstrated a dose-dependent inhibitory effect on eosinophil recruitment into the airways (**Fig. 6B**). Significantly, R321 reduced eosinophil counts in the BALF beginning with a dose of 6 mg/kg (44.24 ± 9.33 % of vehicle) and reached 69.33 ± 4.20% inhibition at the maximum dose of 12 mg/kg (**Fig. 6C**). An IC_{50} value of 8.16 mg/kg was obtained from linear regression analysis. R323 showed no inhibitory effect at 12 mg/kg. No significant differences were observed in total cell counts of other inflammatory cells including macrophages, neutrophils, or lymphocytes (**Supplementary Fig. S6**). MBP1-stained lung tissues showed a 36.20 ± 5.28% decrease in eosinophil counts following treatment with 12 mg/kg of R321 (**Fig. 6D**). In a therapeutic protocol (**Supplementary Fig. S5B**), R321 (12 mg/kg) successfully reduced airway (BAL) eosinophils by 74.18 ± 6.50%. (**Fig. 7A**) and lung eosinophils by 83.30 ± 7.29 %, fully reversing both allergen-induced eosinophilia in the blood (**Fig. 7B**) and in the lung tissue (**Fig. 7C and 7E**) to levels comparable to PBS-sham challenged mice. As expected, blood eosinophils displayed reduced levels of surface CCR3 upon exposure to allergen when compared to sham-challenged controls (~29% reduction) (**Fig. 7D**), and R321 treatment further reduced CCR3 levels (~15% reduction compared to vehicle, p=0.01). The protocols for allergen

(DRA) sensitization, airway challenge, and peptide treatments are provided in **Supplemental Fig. S5**.

R321 blocks airway hyperresponsiveness in allergen-challenged mice

DRA-challenged mice showed a ~9 times higher peak system and airway resistance in response to methacholine as compared to sham-challenged (PBS) mice (**Fig. 6E and Fig. 6F**). R321 treatment had a striking effect on airway responsiveness, reducing both the system and airway pulmonary resistance of challenged mice to levels comparable to those observed in sham-challenged (PBS) mice.

R321 interacts with CCR3 and allows chemokine binding

To study the binding of R321 to CCR3, we used NMR spectroscopy to correlate ^{13}C and ^{1}H frequencies in $^{13}CH_3$ groups of membrane proteins incorporated by reductive methylation (**Supplementary Fig. S7**) [28-33]. The HSQC spectrum of CCR3 positive membranes contained four discernable signals (**Fig. 7A**). In contrast, CCR3 null membrane exhibited only two signals (**Fig. 7A**). These signals overlapped with only two out of four signals of CCR3 positive membranes, suggesting that the remaining two signals belong to CCR3 (**Fig. 7A**). Immunoblotting only detected CCR3 in the CCR3 positive membranes (**Supplementary Fig. S8**). Moreover, CCL11 specifically reduced the intensity of CCR3 signals (**Fig. 7B,** black arrows) but did not affect the spectrum of CCR3 null membranes (**Supplementary Fig. S8**). Similar to CCL11, R321 shifted only

the CCR3 signals (**Fig. 7C**). This suggests that R321 specifically perturbs CCR3 structure. Next, we investigated the interaction of R321 and CCR3 in the presence of CCL11 (**Fig. 7D-F**). The chemical shift changes and differences in signal intensities show that neither CCL11 nor R321 interfere with each other's binding to the receptor. This suggests that R321 and CCL11 interact with CCR3 simultaneously and R321 alters CCL11's ability to activate signaling (**Fig. 7**).

Dose-dependent responses of CCR3 at different concentrations of R321 (**Supplementary Fig. S7 and Fig. S9**) allowed calculation of the dissociation constants (**Supplementary Fig. S7C**). We found two dissociation constants for R321 binding to the receptor, one in the nanomolar range and the other in the micromolar range. This suggests that R321 might employ two distinct mechanisms for interaction with CCR3, potentially explaining its unique inhibitory profiles *in vitro* and *in vivo*.

DISCUSSION

In the present study, we report the development and characterization of a novel peptide inhibitor of CCR3. The described peptide (R321) self-assembles into uniformly sized nanoparticles, essentially functioning as its own carrier and delivery system. Self-assembly protects the peptide from proteolytic degradation, a known issue with peptide-based drugs[20]. Addition of polyethylene glycol (PEG) to the R321 nanoparticles is recognized to further prevent aggregation, proteolytic degradation, improve pharmacokinetics, and reduce immunogenicity of peptide based drugs[34].

In this study, *iv* administration was used as the most reliable method for delivering R321 peptide nanoparticles to the systemic circulation. However, future studies will involve alternative routes of administration, notably formulating R321 preparations for nebulization or direct airway instillation or inhalation. UCB35625, initially identified as a high affinity unbiased antagonist of CCR3 and CCR1, was subsequently found to be an agonist of CCR2 and CCR5, making it prohibitively complex for *in vivo* studies[35, 36]. SB328437 was developed as a specific inhibitor of CCR3 in eosinophils and was shown to successfully suppress OVA-induced accumulation of eosinophils in the lungs of mice adoptively transferred with *in vitro*-differentiated Th2 cells[37, 38]. However, a very high subcutaneous dose (100 mg/kg) of SB328437 resuspended with Tween-80 was used in the study, and we have also experienced solubility issues with this compound, making it unsuitable for *iv* injection.

CCR3 signaling is increasingly implicated in various pathological contexts besides allergic inflammation. These include age-related macular degeneration,[39] reproductive malignancies,[40-42] eosinophilic myocarditis,[43] neurodegenerative diseases,[44] renal cell carcinoma,[45] Crohn's disease,[46] and glioblastoma.[47] Several antagonists that prevent chemokine binding to CCR3 have been developed; however, none of these inhibitors have been FDA approved. Failures of small molecule CCR3 inhibitors in the few clinical trials that have been conducted have called into question the role of CCR3 in airway eosinophilia in asthma, suggesting that CCR3 is not a viable target for drug development. However, a clinical trial of the unbiased CCR3 antagonist, GW766994, showed a trend towards inhibition of sputum eosinophils, with significant inhibition of AHR,[48] suggesting treatment duration may not have been sufficient to meet primary study endpoints,[48, 49] or eosinophils and other CCR3+ target cells developed resistance (tolerance) to this unbiased antagonist. Furthermore, studies have shown that CCR3 knock-out mice display up to a maximum of 70% reduction in eosinophil recruitment into the airways in an OVA-asthma model.[50] In agreement with this finding, our *in vivo* results from the mouse DRA-asthma model also validate CCR3 as a drug target, since the highest prophylactically administered dose of R321 reached ~70% inhibition of eosinophil recruitment into the airways and strikingly, when delivered therapeutically, completely reversed both blood and lung tissue allergen-induced eosinophilia. The inhibitory effect on blood eosinophil numbers could be explained by either R321 blocking egress of eosinophils from the bone marrow and/or decreasing eosinophil differentiation.[51] Further studies are warranted, including in severe chronic murine asthma models. Despite incompletely inhibiting eosinophil recruitment to the airways,

R321 delivered at 12 mg/kg fully blocked the development of AHR to methacholine in allergen-challenged mice. Airway hyperresponsiveness is considered a cardinal feature of asthma, and the ability of R321 to completely antagonize the development of AHR in a robust allergic asthma model offers promise of R321 as a therapeutic agent in the treatment of the eosinophilic asthma phenotype. The presence of CCR3 on other non-eosinophil cells relevant to asthma and airway hyperreactivity, such as basophils and subsets of mast cells and Th2-lymphocytes could indicate a wider therapeutic effect of R321 beyond inhibition of eosinophil recruitment and activation.

Drug development thus far has focused on conventional unbiased antagonists, despite growing evidence that chemokine receptors mediate effects both through G protein and non-G protein effectors. An unbiased antagonist of CCR3 acts to inhibit both the activation branch as well as the desensitization and degradation branch of CCR3 signaling following ligand binding. In this scenario, the cell increases its surface receptor density as the basal turnover process continues to produce new receptors.[52, 53] Receptor accumulation may potentially explain the limited *in vivo* success observed with such unbiased antagonists, e.g. in a clinical trial in subjects with eosinophilic asthma,[48] as eosinophils may eventually overcome inhibition and become resistant.

Our results demonstrate that the novel R321 peptide effectively inhibits G-protein mediated signal transduction by CCR3, but does not interfere with β-arrestin signaling, receptor internalization and degradation (**Supplemental Figure S10**). In contrast, small molecule CCR3 antagonists, UCB35625 and SB328437, partially or completely block

CCR3 internalization, with this effect becoming more pronounced with longer treatment times. Our observation that R321 by itself appears to promote CCR3 internalization, and without acting as an agonist for chemotaxis, suggests the fate of CCR3 internalized in the presence of R321 is biased towards that of degradation instead of cell activation. As demonstrated by NMR studies, both R321 and CCL11 can bind simultaneously and specifically to the CCR3 receptor, and R321 has two independent binding sites. It is possible that R321 binding at a site different than the eotaxin ligand stabilizes a receptor conformation that induces β-arrestin recruitment, although with a much weaker affinity than observed for the eotaxin ligands. Future structural studies should help clarify the unique inhibitory profile of R321.

Avoiding the pitfall of tolerance development by seeking out novel biased antagonists of the CCR3 signaling cascade may hold significant therapeutic promise for eosinophilic asthma, EoE and other eosinophil-associated diseases. Our results should also prove encouraging in a continuing search for biased antagonists of not only CCR3, but also other chemokine receptors, and point the way toward approaches alternative to classical ligand-displacement compounds.

Acknowledgments

We would like to thank Dr. Boris Garnier for his help with initial peptide design and characterization, Dr. Jian Du for his help with AML14.3D10-CCR3 cell line maintenance, cryopreservation and experiments, and Dr. S. Tarasov and M. Dyba (Biophysics Resource, SBL, NCI at Frederick) for assistance with mass spectrometry and DLS

484 measurements. We also thank Dr. James Pease, Imperial College, London, for his
485 provision of the 4DE4-CCR3 cell line used in initial studies of CCR3 transmembrane
486 domain peptide inhibition of CCR3/eotaxin-mediated chemotaxis. This work was
487 supported in part by NIH Grants R21HL118588 (SJA/VG), R01HL126852 (GYP),
488 K01DK106315 (JCM), K24DK100303 (GTF), the LaCache Chair for GI Allergic and
489 Immunologic Diseases (GTF), and a grant from the University of Illinois at Chicago
490 Chancellors Innovation Fund – Proof of Concept program (SJA/VG), and the Intramural
491 Research Program of the National Cancer Institute, NIH (NIT). HA was supported in
492 part by a postdoctoral fellowship from the American Parkinson Disease Association
493 (APDA). The content is solely the responsibility of the authors and does not necessarily
494 represent the official views of the NIH. These funding sources had no involvement in
495 study design; in the collection, analysis and interpretation of data; in the writing of the
496 report; and in the decision to submit the article for publication.

497

REFERENCES

1. Busse W, Sedgwick J. Eosinophils in asthma. Annals of Allergy 1992; 68:286-90.
2. Markowitz JE, Liacouras CA. Eosinophilic esophagitis. Gastroenterology Clinics of North America 2003; 32:949-66.
3. Willems LI, Ijzerman AP. Small molecule antagonists for chemokine CCR3 receptors. Medicinal research reviews 2010; 30:778-817.
4. Pease JE, Horuk R. Recent progress in the development of antagonists to the chemokine receptors CCR3 and CCR4. Expert opinion on drug discovery 2014; 9:467-83.
5. Stellato C, Brummet M, Plitt J, Shahabuddin S, Baroody F, Liu M, et al. Expression of the C-C chemokine receptor CCR3 in human airway epithelial cells. Journal of Immunology 2001; 166:1457-61.
6. Kampen G, Stafford S, Adachi T, Jinquan T, Quan S, Grant J, et al. Eotaxin induces degranulation and chemotaxis of eosinophils through the activation of ERK2 and p38 mitogen-activated protein kinases. Blood 2000; 15:1911-7.
7. Zhu Y, Bertics P. Chemoattractant-induced signaling via the Ras-ERK and PI3K-Akt networks, along with leukotriene C4 release, is dependent on the tyrosine kinase Lyn in IL-5- and IL-3-primed human blood eosinophils. Jornal of Immunology 2011; 186:516-26.
8. Zimmermann N, Conkright JJ, Rothenberg ME. CC chemokine receptor-3 undergoes prolonged ligand-induced internalization. The Journal of biological chemistry 1999; 274:12611-8.

519 9. Zimmermann N, Rothenberg ME. Receptor internalization is required for eotaxin-
520 induced responses in human eosinophils. The Journal of allergy and clinical immunology
521 2003; 111:97-105.
522 10. Meiser A, Mueller A, Wise EL, McDonagh EM, Petit SJ, Saran N, et al. The Chemokine
523 Receptor CXCR3 Is Degraded following Internalization and Is Replenished at the Cell
524 Surface by De Novo Synthesis of Receptor. The Journal of Immunology 2008; 180:6713-
525 24.
526 11. Fulkerson PC, Fischetti CA, McBride ML, Hassman LM, Hogan SP, Rothenberg ME. A
527 central regulatory role for eosinophils and the eotaxin/CCR3 axis in chronic
528 experimental allergic airway inflammation. Proceedings of the National Academy of
529 Sciences of the United States of America 2006; 103:16418-23.
530 12. Ying S, Robinson DS, Meng Q, Rottman J, Kennedy R, Ringler DJ, et al. Enhanced
531 expression of eotaxin and CCR3 mRNA and protein in atopic asthma. Association with
532 airway hyperresponsiveness and predominant co-localization of eotaxin mRNA to
533 bronchial epithelial and endothelial cells. European journal of immunology 1997;
534 27:3507-16.
535 13. Uy GL, Retting MP, Motabi IH, McFarland K, Trinkaus kM, Hladnik LM, et al. A phase 1/2
536 study of chemosensitization with the CXCR4 antagonist plerixafor in relapsed or
537 refractory acute myeloid leukemia. Blood 2012; 119:3917-24.
538 14. Sison EAR, Magoon D, Li L, Annesley CE, Romagnoli B, Douglas GJ, et al. POL5551, a
539 novel and potent CXCR4 antagonist, enhances sensitivity to chemotherapy in pediatric
540 ALL. Oncotarget 2015; 6:30902-18.

15. Schmid CL, Kennedy NM, Ross NC, Lovell KM, Yue Z, Morgenweck J, et al. Bias Factor and Therapeutic Window Correlate to Predict Safer Opioid Analgesics. Cell 2017; 171:1165-75.

16. Daugherty BL, Siciliano SJ, DeMartino JA, Malkowitz L, Sirotina A, Springer MS. Cloning, Expression, and Characterization of the Human Eosinophil Eotaxin Receptor Journal of Experimental Medicine 1996; 183:2349-54.

17. Goplen N, Karim MZ, Liang Q, Gorska MM, Rozario S, Guo L, et al. Combined sensitization of mice to extracts of dust mites, ragweed and aspergillus breaks through tolerance and establishes chronic features of asthma in mice. Journal of Allergy and Clinical Immunology 2009; 123:925-32.

18. Denzler KL, Borchers MT, Crosby JR, Cieslewicz G, Hines EM, Justice JP, et al. Extensive Eosinophil Degranulation and Peroxidase-Mediated Oxidation of Airway Proteins Do Not Occur in a Mouse Ovalbumin-Challenge Model of Pulmonary Inflammation. The Journal of Immunology 2001; 167:1672-82.

19. Tarasov SG, Gaponenko V, Howard OM, Chen Y, Oppenheim JJ, Dyba MA, et al. Structural plasticity of a transmembrane peptide allows self-assembly into biologically active nanoparticles. Proc Natl Acad Sci U S A; 108:9798-803.

20. Lee Y, Chen Y, Tarasova NI, Gaponenko V. The structure of monomeric components of self-assembling CXCR4 antagonists determines the architecture of resulting nanostructures. Nanotechnology 2011; 22:505101.

21. Fujisawa T, Kato Y, Nagase H, Atsuta J, Terada A, Iguchi K, et al. Chemokines induce eosinophil degranulation through CCR-3. Journal of Allergy and Clinical Immunology 2000; 106:507-13.

22. Kumari P, Srivastava A, Banerjee R, Ghosh E, Gupta P, Ranjan R, et al. Functional competence of a partially engaged GPCR–β-arrestin complex. Nature Communications 2016; 7:13416.

23. Ahn S, Shenoy SK, Wei H, Lefkowitz RJ. Differential kinetic and spatial patterns of beta-arrestin and G protein-mediated ERK activation by the angiotensin II receptor. Journal of Biological Chemistry 2004; 279:35518–25.

24. Shenoy SK, Drake MT, Nelson CD, Houtz DA, Xiao K, Madabushi S, et al. β-Arrestin-dependent, G Protein-independent ERK1/2 Activation by the β2 Adrenergic Receptor. The Journal of biological chemistry 2006; 281:1261-73, .

25. Lefkowitz RJ, Shenoy SK. Transduction of Receptor Signals by ß-Arrestins. Science 2005; 308:512-7.

26. Rajagopal S, Kim J, Ahn S, Craig S, Lam CM, Gerard NP, et al. β-arrestin- but not G protein-mediated signaling by the "decoy" receptor CXCR7. Proc Natl Acad Sci U S A 2010; 107:628-32.

27. Wise EL, Bonner KT, Williams TJ, Pease JE. A single nucleotide polymorphism in the CCR3 gene ablates receptor export to the plasma membrane. The Journal of allergy and clinical immunology 2010; 126:150-7.e2.

28. Chavan TS, Abraham S, Gaponenko V. Application of reductive (1)(3)C-methylation of lysines to enhance the sensitivity of conventional NMR methods. Molecules 2013; 18:7103-19.

29. Abraham SJ, Hoheisel S, Gaponenko V. Detection of protein-ligand interactions by NMR using reductive methylation of lysine residues. J Biomol NMR 2008; 42:143-8.

30. Abraham SJ, Kobayashi T, Solaro RJ, Gaponenko V. Differences in lysine pKa values may be used to improve NMR signal dispersion in reductively methylated proteins. J Biomol NMR 2009; 43:239-46.

31. Tripathi A, Vana PG, Chavan TS, Brueggemann LI, Byron KL, Tarasova NI, et al. Heteromerization of chemokine (C-X-C motif) receptor 4 with alpha1A/B-adrenergic receptors controls alpha1-adrenergic receptor function. Proc Natl Acad Sci U S A 2015; 112:E1659-68.

32. Sounier R, Mas C, Steyaert J, Laeremans T, Manglik A, Huang W, et al. Propagation of conformational changes during mu-opioid receptor activation. Nature 2015; 524:375-8.

33. Bokoch MP, Zou Y, Rasmussen SG, Liu CW, Nygaard R, Rosenbaum DM, et al. Ligand-specific regulation of the extracellular surface of a G-protein-coupled receptor. Nature 2010; 463:108-12.

34. Harris J, Chess R. Effect of pegylation on pharmaceuticals. Nature reviews. Drug discovery 2003; 2:214-21.

35. Sabroe I, Peck MJ, Keulen BJV, Jorritsma A, Simmons G, Clapham PR, et al. A Small Molecule Antagonist of Chemokine Receptors CCR1 and CCR3. Potent Inhibition of

Eosinophil Function and CCR3-mediated HIV-1 Entry. The Journal of Biological Chemistry 2000; 275:25985-92.

36. Corbisier J, Huszagh A, Gales C, Parmentier M, Springael J-Y. Partial Agonist and Biased Signaling Properties of the Synthetic Enantiomers J113863/UCB35625 at Chemokine Receptors CCR2 and CCR5. The Journal of Biological Chemistry 2017; 292:575-84.

37. John R. White, Judithann M. Lee, Kimberly Dede, Christina S. Imburgia, Anthony J. Jurewicz, George Chan, et al. Identification of potent, selective non-peptide CCR3 antagonist that inhibits eotaxin-, eotaxin-2 and MCP-4 induced eosinophil migration. The Journal of biological chemistry 2000; 275:36626-31.

38. Mori A, Ogawa K, Someya K, Kunori Y, Nagakubo D, Yoshie O, et al. Selective suppression of Th2-mediated airway eosinophil infiltration by low-molecular weight CCR3 antagonists. International Immunology 2007; 19:913-21.

39. Takeda A, Baffi JZ, Kleinman ME, Cho WG, Nozaki M, Yamada K, et al. CCR3 is a target for age-related macular degeneration diagnosis and therapy. Nature 2009; 460:225-30.

40. Long H, Xie R, Xiang T, Zhao Z, Lin S, Liang Z, et al. Autocrine CCL5 signaling promotes invasion and migration of CD133+ ovarian cancer stem-like cells via NF-κB-mediated MMP-9 upregulation. Stem cells (Dayton, Ohio) 2012; 30:2309-19.

41. Agarwal M, He C, Siddiqui J, Wei JT, Macoska JA. CCL11 (eotaxin-1): a new diagnostic serum marker for prostate cancer. The Prostate 2013; 73:573-81.

42. Zhu F, Liu P, Li J, Zhang Y. Eotaxin-1 promotes prostate cancer cell invasion via activation of the CCR3-ERK pathway and upregulation of MMP-3 expression. Oncology reports 2014; 31:2049-54.

43. Diny NL, Hou X, Barin JG, Chen G, Talor MV, Schaub J, et al. Macrophages and cardiac fibroblasts are the main producers of eotaxins and regulate eosinophil trafficking to the heart. Eur J Immunol 2016.

44. Huber AK, Giles DA, Segal BM, Irani DN. An emerging role for eotaxins in neurodegenerative disease. Clin Immunol 2016.

45. Jöhrer K, Zelle-Rieser C, Perathoner A, Moser P, Hager M, Ramoner R, et al. Up-regulation of functional chemokine receptor CCR3 in human renal cell carcinoma. Clinical Cancer Research 2005; 11:2459-65.

46. Masterson JC, McNamee EN, Jedlicka P, Fillon S, Ruybal J, Hosford L, et al. CCR3 Blockade Attenuates Eosinophilic Ileitis and Associated Remodeling. Am J Pathol 2011; 179:2302-14.

47. Tian M, Chen L, Ma L, Wang D, Shao B, Wu J, et al. Expression and prognostic significance of CCL11/CCR3 in glioblastoma. Oncotarget 2016; 7:32617-27.

48. Neighbour H, Boulet L-P, Lemiere C, Sehmi R, Leigh R, Sousa AR, et al. Safety and efficacy of an oral CCR3 antagonist in patients with asthma and eosinophilic bronchitis: a randomized, placebo-controlled clinical trial. Clinical and experimental allergy : journal of the British Society for Allergy and Clinical Immunology 2014; 44:508-16.

49. Thomson NC. Novel therapies targeting eosinophilic inflammation in asthma. Clinical and experimental allergy : journal of the British Society for Allergy and Clinical Immunology 2014; 44:462-8.

644 50. Humbles AA, Lu B, Friend DS, Okinaga S, Lora J, Al-garawi A, et al. The murine CCR3
645 receptor regulates both the role of eosinophils and mast cells in allergen-induced airway
646 inflammation and hyperresponsiveness. Proc Natl Acad Sci U S A 2001; 99:1479- 84.
647 51. Lamkhioued B, Abdelilah SG, Hamid Q, Mansour N, Delespesse G, Renzi PM. The CCR3
648 receptor is involved in eosinophil differentiation and is up-regulated by Th2 cytokines in
649 CD34+ progenitor cells. Journal of Immunology 2003; 171:537-47.
650 52. Paradisa JS, Lya S, Blondel-Tepaza É, Galana JA, Beautraita A, Scottd MGH, et al.
651 Receptor sequestration in response to β-arrestin-2 phosphorylation by ERK1/2 governs
652 steady-state levels of GPCR cell-surface expression. Proc Natl Acad Sci U S A 2015;
653 112:E5160–E8.
654 53. Allouche S, Noble F, Marie N. Opioid receptor desensitization: mechanisms and its link
655 to tolerance. Frontiers in Pharmacology 2014; 5:1-6.

656

657 **FIGURE LEGENDS**

658

659 **Figure 1. The R321 CCR3 peptide and its scrambled control (R323) self-assemble**
660 **into nanoparticles. (A)** Structures of R321 and the scrambled peptide R323. Alignment
661 with human and mouse CCR3 shows a high degree of identity at the TM2 region. **(B)**
662 Dynamic Light Scattering (DLS) regularization distribution histograms are shown for 10
663 µM peptide solutions in PBS. Radii for R321 and R323 are 7.1 ± 0.7 nm and 4.5 ± 0.4
664 nm, respectively, with R323 somewhat smaller and more polydisperse; the
665 polydispersity index of R321 and R323 were 0.07 and 0.28, respectively. Results
666 represent mean ± SEM from experiments (n=3) performed in duplicate **(C**). R321 self-
667 assembly into nanoparticles shows no dependence on peptide concentration. TM:
668 transmembrane. ECL: extracellular loop.

669

670 **Figure 2. R321 inhibits eotaxin/CCR3-mediated chemotaxis.** R321 (0.001-10 µM)
671 dose-response inhibition of chemotaxis induced by CCL11/Eotaxin-1 (12nM),
672 CCL24/Eotaxin-2 (20nM), and CCL26/Eotaxin-3 (100nM) for 4h of **(A)** blood eosinophils
673 and **(B)** AML14.3D10-CCR3 cells. **(C)** IC_{50}/IC_{90} inhibitory activity of the R321 peptide on
674 eotaxin-induced chemotaxis of blood eosinophils. **(D)** Scrambled peptide control – R323
675 (1 µM) does not significantly inhibit chemotaxis of blood eosinophils. In contrast, R321
676 inhibits chemotaxis by >90% when tested at the same (1 µM) concentration. **(E)** R321
677 does not inhibit CXCL12/CXCR4-mediated chemotaxis of Jurkat-T lymphocytic
678 leukemia cells. Results are normalized to % maximum chemotactic response and are

679 representative of the mean ± SEM from experiments (n=3) performed in triplicate.
680 ns=*p*>0.05.
681
682 **Figure 3. (A) R321 inhibits activation of pertussis toxin (PT) sensitive $G_{\alpha i}$.**
683 AML14.3D10-CCR3 cells were pretreated with PT (200 ng/mL) or R321 (10 µM) before
684 being stimulated with CCL11 (12 nM) for 1 min. Active, GTP-bound Gαi was
685 immunoprecipitated using antibody specific for $G\alpha i_{GTP}$ and detected by western blotting
686 using antibody to total Gαi. The input lysates were blotted for CCR3 as a loading
687 control. **(B) R321 does not inhibit β-arrestin signaling by activated CCR3.**
688 AML14.3D10-CCR3 cells were treated with CCL11 (12 nM) or RANTES/CCL5 (12 nM)
689 for 3h. Decrease in CCR3 indicates receptor degradation after exposure to ligand.
690 Pretreatment with 10 µM R321 before CCR3 ligands enhances degradation. **(C)**
691 **Eotaxin-mediated activation of CCR3 leads to biphasic activation of AKT.** After
692 CCR3 activation by the indicated chemokines (12 nM), biphasic phosphorylation of AKT
693 was observed. Acute (2min) phosphorylation is mediated by G protein signaling. Late
694 phase (30min) phosphorylation is likely due to β-arrestin signaling.
695
696 **Figure 4. R321 does not inhibit ligand-induced β-arrestin recruitment and**
697 **signaling by activated CCR3. (A)** Following CCR3 activation with 100 nM CCL11,
698 biphasic ERK1/2 phosphorylation was observed. Acute (2-5min) phosphorylation is
699 mediated by G protein signaling. Late phase (30min) phosphorylation is likely due to β-
700 arrestin signaling. R321 (10µM) inhibits only acute phosphorylation of ERK1/2.
701 Scrambled peptide control – R323 (10µM) does not inhibit acute or late phase

phosphorylation. SB328437 (10μM) inhibits both acute and late phase phosphorylation and UCB35625 (10μM) inhibits the late phase to a higher degree than the early phase. **(B)** Representative confocal images of AML14.3D10-CCR3 cells exposed to vehicle or inhibitors for 30 min and stimulated with CCL11/eotaxin-1 for 30 min. **(C)** Quantitation by Pearson's correlation method shows colocalization of CCR3 to β-arrestin2 30 min after stimulation with CCL11/eotaxin-1. R321 and R323 (10 μM) did not inhibit CCL11-induced β-arrestin2 recruitment to CCR3 whereas the CCR3 antagonist SB328437 and UCB35625 strongly inhibited colocalization. Results represent mean (50 cells per treatment group) ± SEM from 3 independent experiments. ($^{*}p \leq 0.05$, $^{**}p \leq 0.01$, $^{****}p \leq 0.0001$ as compared to control).

Figure 5. R321 does not inhibit CCL11-induced CCR3 internalization and does not induce resistance (tolerance) to inhibition of CCL11-induced chemotaxis. (A) R321 does not inhibit CCL11-mediated internalization of CCR3. When added concurrently with 12 nM CCL11, R321 (1μM) and R323 (1μM) did not interfere with CCL11-induced receptor internalization. Both SB328437 (1 μM) and UCB35625 (1 μM) significantly inhibited the chemokine's ability to induce CCR3 internalization. **(B)** R321 alone decreases CCR3 surface expression**.** R321 dose-response reduction of surface CCR3 expression on AML14.3D10-CCR3 cells. Significant internalization levels were reached at 1μM R321. **(C)** R321 maintains prolonged inhibitory activity. AML14.3D10-CCR3 cells were treated for 24h, 48h or 72h with R321 or unbiased antagonists (all at 1 μM) ± CCL11 (12 nM). **(D)** R321 promotes CCR3 internalization in human blood eosinophils over a prolonged incubation period. Results shown as surface expression of

CCR3 as percentage of vehicle expression. Of note, SB328437, when used at equimolar concentrations to R321 and UCB35625 (1µM), was a less effective inhibitor of CCL11/CCR3-mediated chemotaxis and failed to promote CCR3 cell surface accumulation. Results represent mean ± SEM from experiments (n=3) performed in triplicate. Compared to vehicle (B, D) or 24h data point (C): *$p \leq 0.05$, **$p \leq 0.01$, ***$p<0.001$, ****$p \leq 0.0001$; Error bars = SEM.

Figure 6. Prophylactic treatment with R321 significantly reduces eosinophil recruitment into the lung airspaces. (A) The DRA-allergen challenge induces a robust eosinophilic response in female BALB/cJ mice as demonstrated by increased numbers of eosinophils in the BAL fluid. **(B)** Total eosinophil cell numbers ($x10^5$) in the BAL fluid show that R321 significantly inhibits eosinophil recruitment into the lung airspaces starting at an *iv* dose of 6 mg/kg. **(C)** The inhibitory effect of R321 is dose-dependent and reaches 69.33 ± 4.20% inhibition at 12 mg/kg. **(D)** Lungs were stained with anti-mMBP1 antibody to identify eosinophils. R321 (12 mg/kg) treatment reduces lung tissue eosinophil counts by 36.20 ± 5.28%. Results are displayed as % of mMBP1 positive cells as compared to total nucleated cells. The mean ± SEM are shown for 6-7 mice/treatment group from 3 independent experiments. R321 at 12 mg/kg significantly lowers respiratory system **(E)** and airway **(F)** responsiveness to methacholine as compared to vehicle or R323 controls. There is no significant difference between R321 treated and sham-challenged mice (n=5, except PBS group where n=4). (****$p<0.0001$, ***$p<0.001$,**$p<0.01$, *$p<0.05$, ^{ns} not significant).

Figure 7. Therapeutic treatment with R321 attenuates established asthmatic lung and airway inflammation in allergen-sensitized/challenged mice. (A) R321 administered at 12 mg/kg inhibits recruitment of eosinophils to the lung airspaces by 74.18 ± 6.50%. **(B)** DRA-allergen challenged mice (Vh) develop significant blood eosinophilia as compared to sham-challenged mice (PBS). Treatment with R321 reduces blood eosinophil numbers to levels not significantly different than those observed in allergen sensitized/PBS-sham challenged mice. **(C)** Following therapeutic treatment with 12 mg/kg of R321, lungs stained for MBP1 positive cells showed tissue eosinophil counts not significantly different from the PBS-sham challenged mice, an 83.30 ± 7.29 % reduction compared to vehicle control. Results are expressed as % MBP1 positive cells compared to total nucleated cells. **(D)** Surface expression of CCR3 in blood eosinophils is reduced upon allergen challenge. R321 does not inhibit CCR3 internalization, but has a promoting effect (vehicle MFI of 13.7 vs. R321-treated group MFI of 11.7, p=0.01). The mean ± SEM is shown for 5 mice/treatment group. (****p<0.0001, ***p<0.001,**p<0.01, *p <0.05,^{ns} not significant). **(E)** Representative images of mouse lung airways (top) and blood vessels (bottom) from Fig. 7C immunostained with HRP-conjugated antibodies to MBP1 (positive cells are dark brown). Black bars represent 100 µm.

Figure 8. R321 binds CCR3 in plasma membrane in the presence of CCL11. ^{13}C HSQC spectra of ^{13}C-reductively methylated CCR3 positive and CCR3 null membranes were recorded with/without 1 µM CCL11 in the presence/absence of 2 µM R321. Spectral comparisons between **(A)** CCR3 (CCR3-K-di$^{13}CH_3$)(red) and CCR3 null

771 membranes (blue); **(B)** CCR3 alone (CCR3-K-di$^{13}CH_3$) (red) and CCR3 + CCL11 (blue);
772 **(C)** CCR3 alone (CCR3-K-di$^{13}CH_3$) (red) and CCR3 + R321 (blue); **(D)** CCR3 alone
773 (CCR3-K-di$^{13}CH_3$) (red) and CCR3 + CCL11 and R321 (blue); **(E)** CCR3 + CCL11 (red)
774 and CCR3 + CCL11 and R321 (blue); and **(F)** CCR3 + R321 (red) and CCR3 + CCL11
775 and R321 (blue) show line-broadening and chemical shift changes indicative of binding.
776 Black arrows show significant changes in CCR3-associated signals, but not in the
777 signals that belong to other membrane proteins.

Figure 1

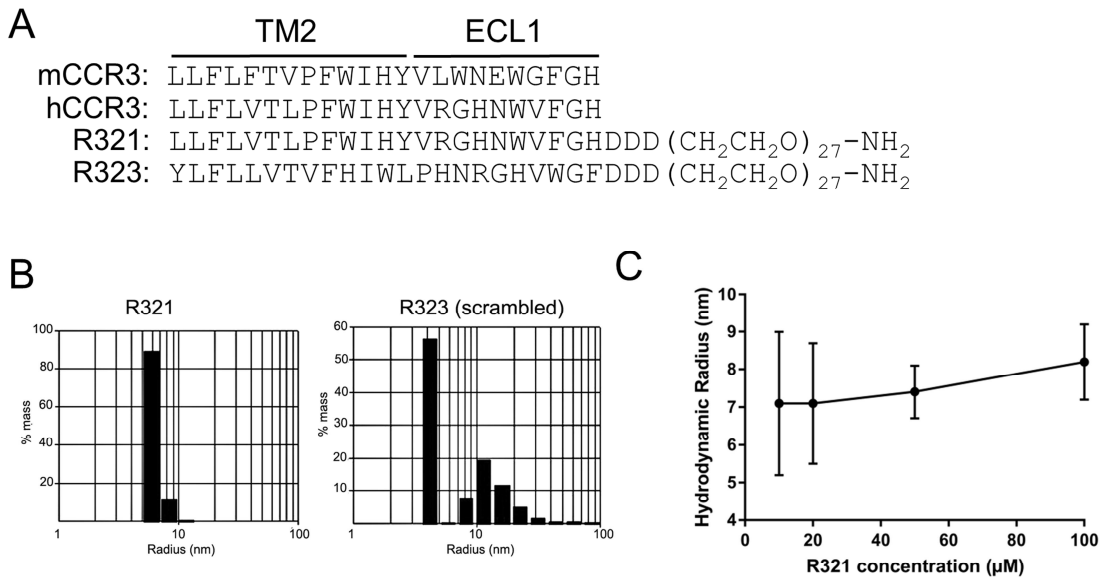
A
TM2
ECL1
mCCR3: LLFLFTVPFWIHYVLWNEWGFGH
hCCR3: LLFLVTLPFWIHYVRGHNWVFGH
R321: LLFLVTLPFWIHYVRGHNWVFGHDDD(CH2CH2O)27-NH2
R323: YLFLLVTVFHIWLPHNRGHVWGFDDD(CH2CH2O)27-NH2
B
R321
R323 (scrambled)
% mass
Radius (nm)
C
Hydrodynamic Radius (nm)
R321 concentration (μM)

Figure 2

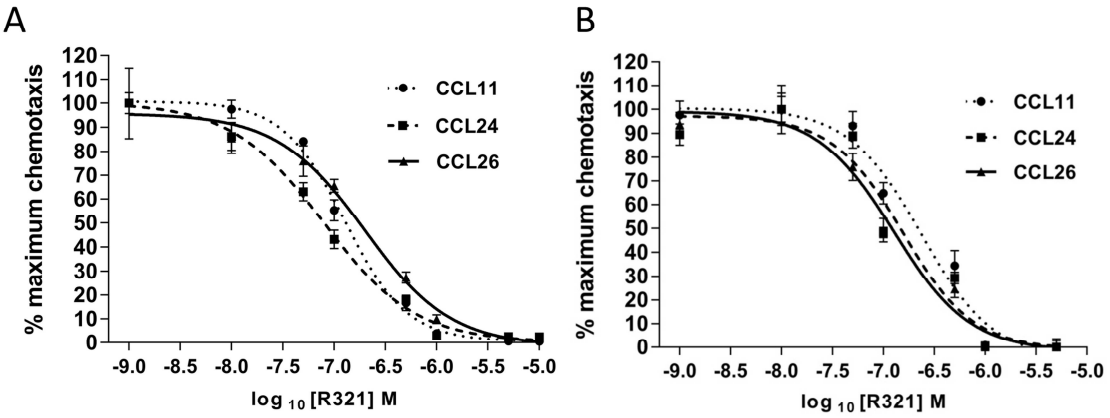

C

	Blood eosinophils		AML14.3D10-CCR3 cells	
	IC_{50} (nM)	IC_{90} (nM)	IC_{50} (nM)	IC_{90} (nM)
CCL11	112.4 ± 10.1	764.7 ± 102.9	212.8 ± 43.7	1746.6 ± 207.2
CCL24	78.9 ± 11.1	733.6 ± 144.1	140.5 ± 22.3	892.8 ± 119.2
CCL26	164.5 ± 20.4	1099.7 ± 151.9	101.7 ± 10.8	779.1 ± 105.1

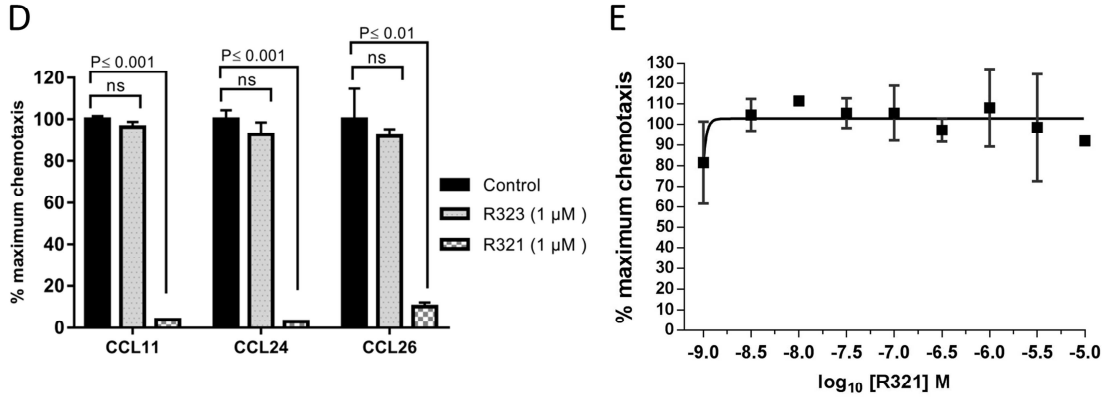

Figure 3

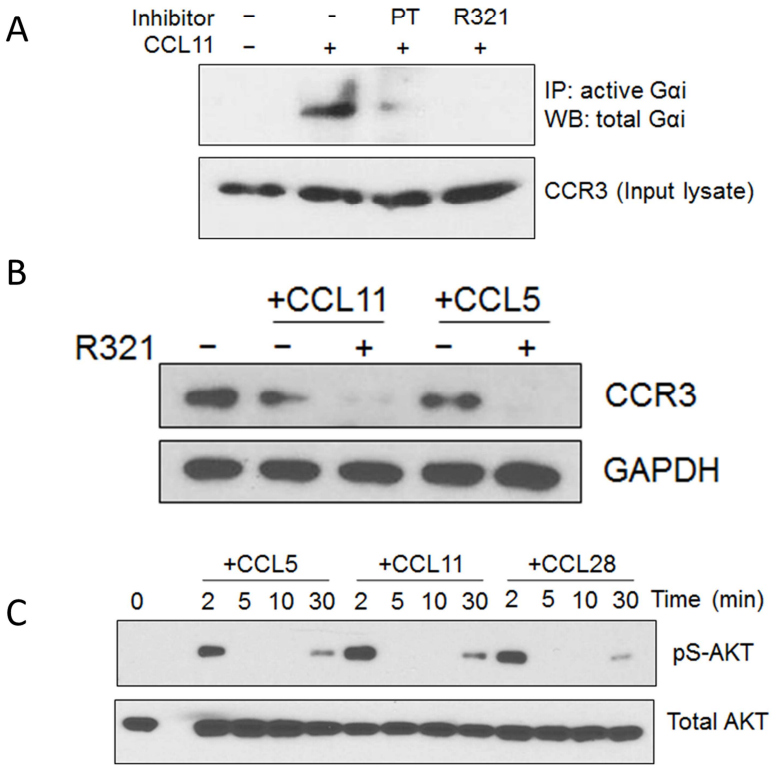
A
Inhibitor – - PT R321
CCL11 – + + +
IP: active Gαi
WB: total Gαi
CCR3 (Input lysate)
B
+CCL11 +CCL5
R321 – – + – +
CCR3
GAPDH
C
+CCL5 +CCL11 +CCL28
0 2 5 10 30 2 5 10 30 2 5 10 30 Time (min)
pS-AKT
Total AKT

Figure 4

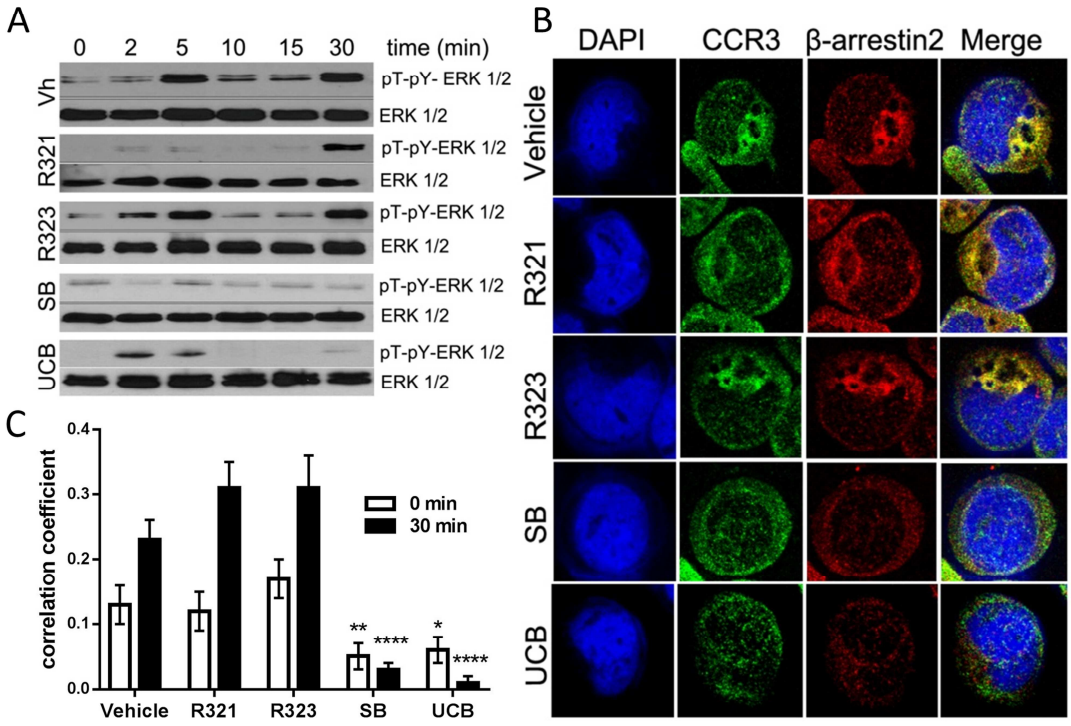
A
0
2
5
10
15
30
time (min)
Vh
pT-pY- ERK 1/2
ERK 1/2
R321
pT-pY-ERK 1/2
ERK 1/2
R323
pT-pY-ERK 1/2
ERK 1/2
SB
pT-pY-ERK 1/2
ERK 1/2
UCB
pT-pY-ERK 1/2
ERK 1/2
B
DAPI
CCR3
β-arrestin2
Merge
Vehicle
R321
R323
SB
UCB
C
correlation coefficient
0.4
0.3
0.2
0.1
0.0
0 min
30 min
**
****
*
****
Vehicle
R321
R323
SB
UCB

Figure 5

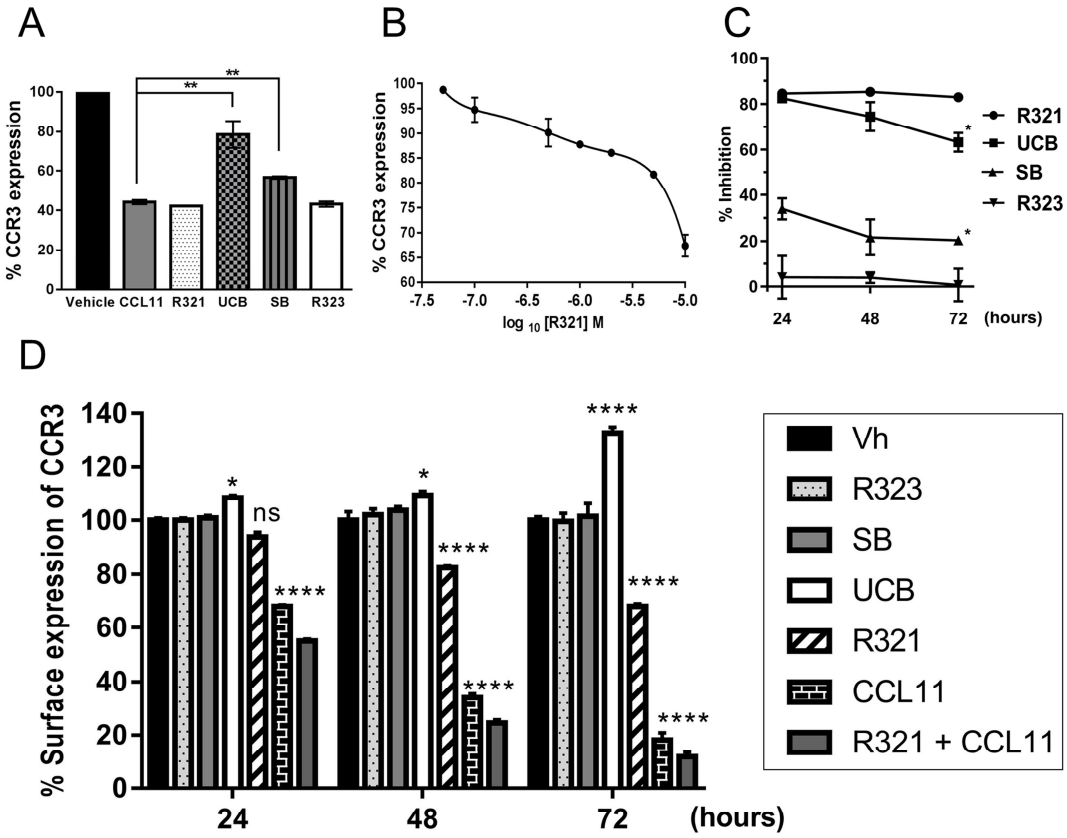
A
% CCR3 expression
Vehicle CCL11 R321 UCB SB R323
B
% CCR3 expression
log 10 [R321] M
C
% Inhibition
R321
UCB
SB
R323
24 48 72 (hours)
D
% Surface expression of CCR3
24 48 72 (hours)
Vh
R323
SB
UCB
R321
CCL11
R321 + CCL11

Figure 6

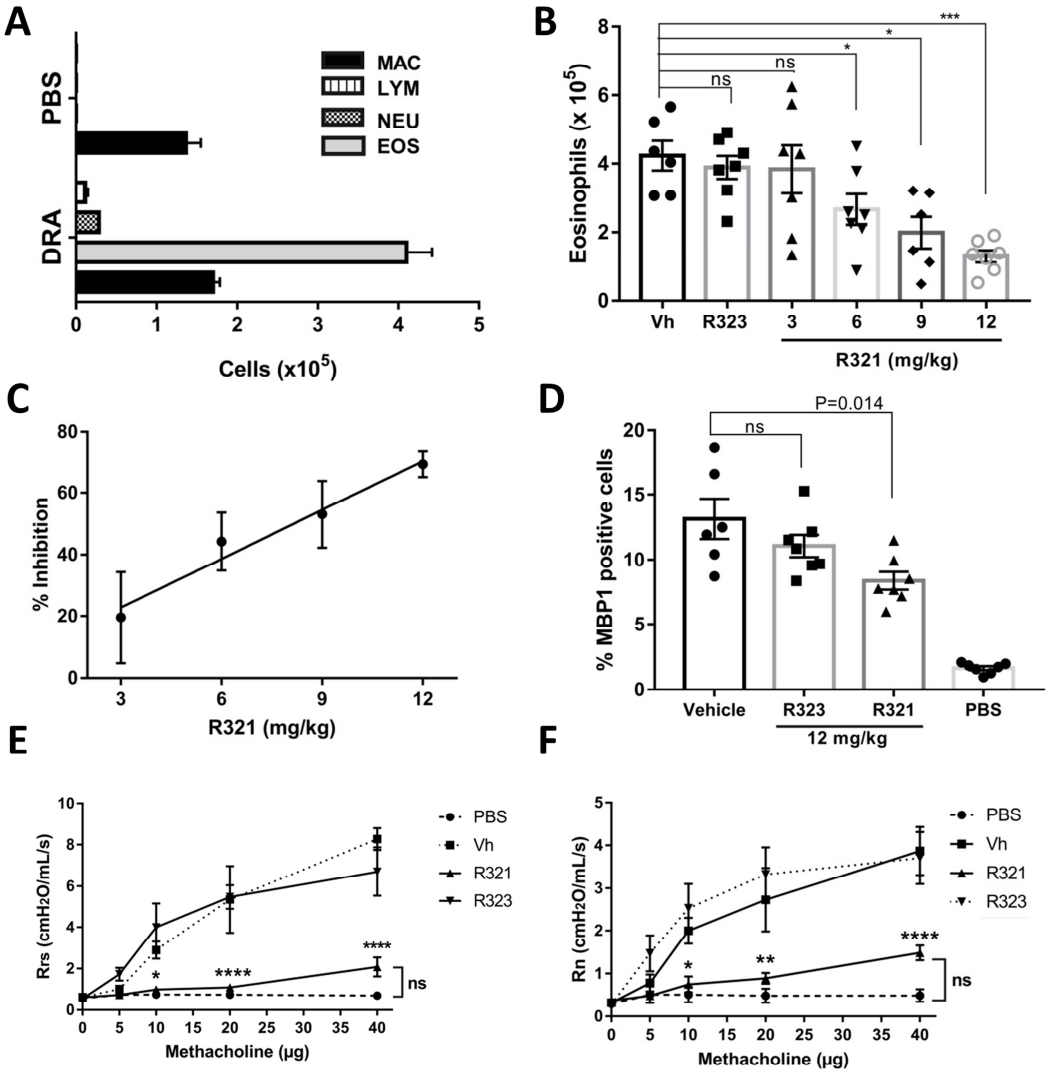
A
PBS
DRA
MAC
LYM
NEU
EOS
0 1 2 3 4 5
Cells (x10^5)
B
Eosinophils (x 10^5)
ns
ns
*
*
***
Vh R323 3 6 9 12
R321 (mg/kg)
C
% Inhibition
0 20 40 60 80
3 6 9 12
R321 (mg/kg)
D
% MBP1 positive cells
P=0.014
ns
0 5 10 15 20
Vehicle R323 R321 PBS
12 mg/kg
E
Rrs (cmH2O/mL/s)
PBS
Vh
R321
R323
*
****
****
ns
0 5 10 15 20 25 30 35 40
Methacholine (µg)
F
Rn (cmH2O/mL/s)
PBS
Vh
R321
R323
*
**
****
ns
0 5 10 15 20 25 30 35 40
Methacholine (µg)

Figure 7

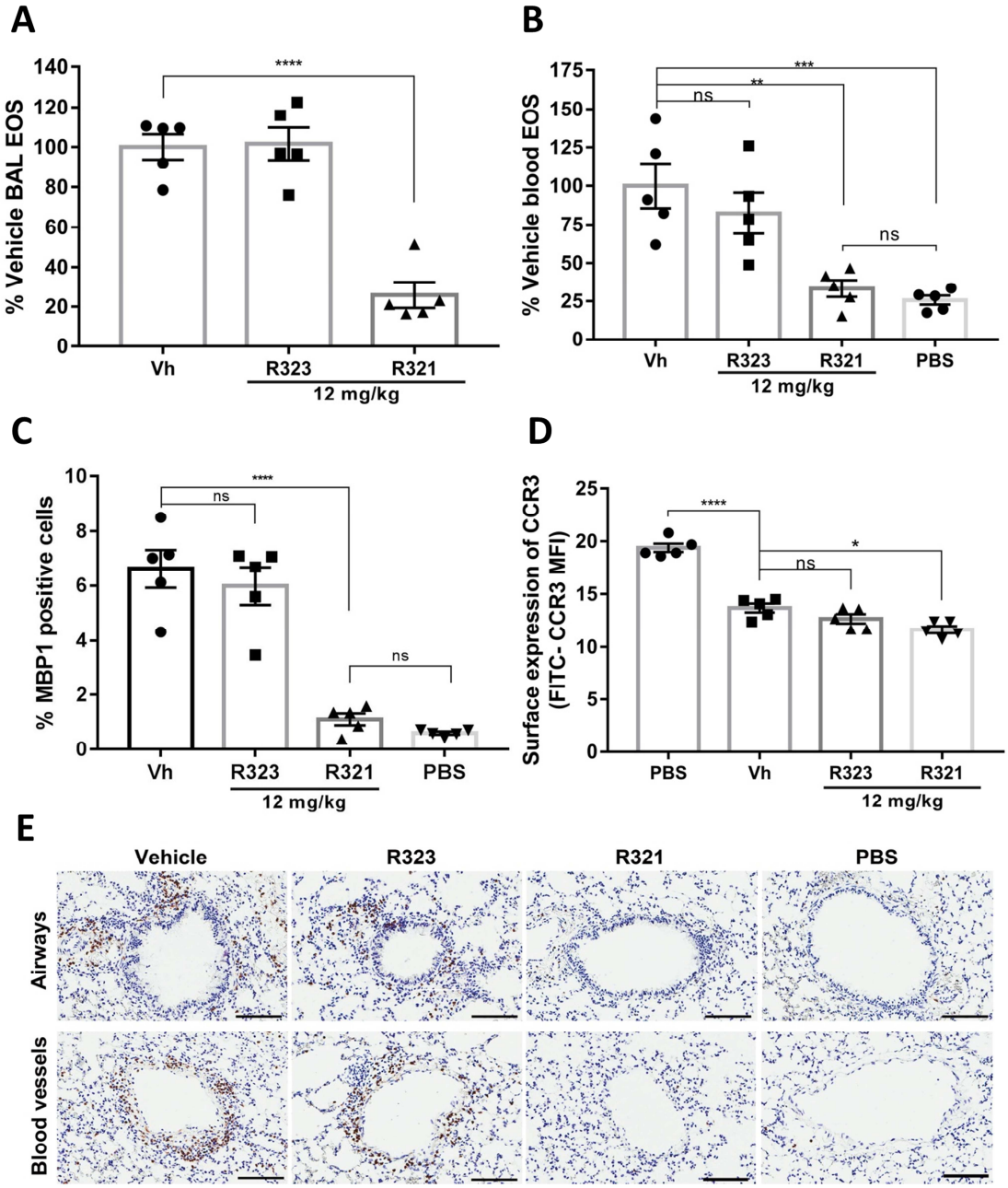
A
% Vehicle BAL EOS
140
120
100
80
60
40
20
0
****
Vh
R323
R321
12 mg/kg
B
% Vehicle blood EOS
175
150
125
100
75
50
25
0
***
**
ns
ns
Vh
R323
R321
PBS
12 mg/kg
C
% MBP1 positive cells
10
8
6
4
2
0
****
ns
ns
Vh
R323
R321
PBS
12 mg/kg
D
Surface expression of CCR3 (FITC- CCR3 MFI)
25
20
15
10
5
0
****
*
ns
PBS
Vh
R323
R321
12 mg/kg
E
Vehicle
R323
R321
PBS
Airways
Blood vessels

Figure 8

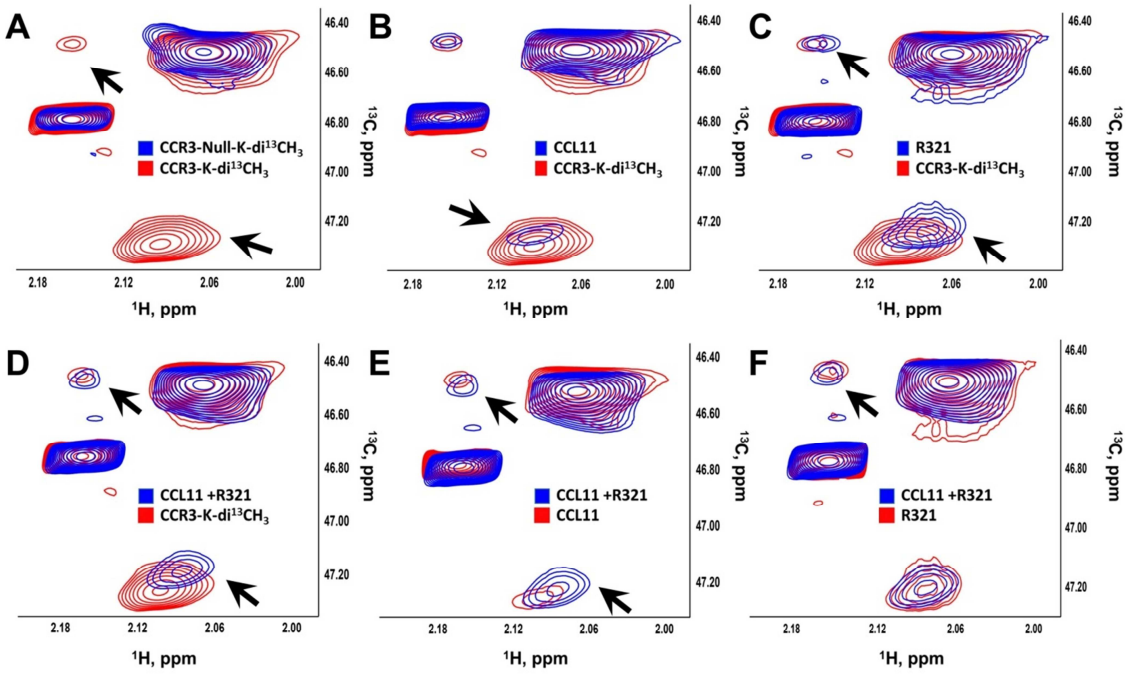
A
CCR3-Null-K-di13CH3
CCR3-K-di13CH3
B
CCL11
CCR3-K-di13CH3
C
R321
CCR3-K-di13CH3
D
CCL11 +R321
CCR3-K-di13CH3
E
CCL11 +R321
CCL11
F
CCL11 +R321
R321
13C, ppm
1H, ppm
46.40
46.60
46.80
47.00
47.20
2.18
2.12
2.06
2.00

Supplemental Materials

MATERIALS AND METHODS

Peptides synthesis and stock preparation

R321 and R323 were synthesized on a Liberty Blue Microwave peptide synthesizer (CEM Corporation) using Fmoc chemistry and low loading Rink Amide MBHA resin (Merck). The following modifications have been introduced to the published protocol of high efficiency peptide synthesis (http://www.ncbi.nlm.nih.gov/pubmed/24456219): The coupling with N,N'-Diisopropylcarbodiimide (DIC)/ ethyl 2-cyano-2-(hydroxyimino) acetate (OXYMA) was performed for 4 min at 90^{o}C for all residue except for His, for which the reaction was carried out for 10 min at 50^{o}C. A 5-fold amino acid excess was used on all cycles and all residues were double-coupled. All deprotection cycles were conducted at room temperature to avoid racemization and aspartimide formation. Due to the high cost of Fmoc-NH-$(PEG)_{27}$-COOH (Merck), it was attached manually overnight using 1.2-fold excess and HCTU as an activating agent. The peptides were cleaved from the resin and deprotected with a mixture of 90.0% (v/v) trifluoroacetic acid (TFA) with 2.5% water, 2.5% triisopropyl-silane, 2.5% 2,2′-(ethylenedioxy)diethanethiol and 5% thioanisol. Peptides were purified on a preparative (25 mm × 250 mm) Atlantis C3 reverse phase column (Agilent Technologies) in a 90 min gradient of 0.1% (v/v) trifluoroacetic acid in water and 0.1% trifluoroacetic acid in acetonitrile, with a 10 mL/min flow rate. The fractions containing peptides were analyzed on Agilent 6100 LC/MS spectrometer with the use of a Zorbax 300SB-C3 PoroShell column and a gradient of 5% acetic acid in water and acetonitrile. Fractions that were more than 95% pure were

combined and freeze dried. Peptides stock solution was prepared by dissolving in DMSO or DMSO-d_6 (for NMR experiments). Upon reconstitution in PBS, pH 7.2, the final concentration of DMSO was less than 1%. The solutions were sonicated, kept at room temperature overnight, centrifuged and stored at -20ºC.

Dynamic Light Scattering (DLS)

Peptides were resuspended in 100% DMSO to a concentration of 1 mM and then further diluted in PBS to a final concentration of 10 µM. The hydrodynamic radius of the peptides was measured on a DynaPro-801 (Protein Solutions, Charlottesville, VA) molecular size detector and the data was analyzed with the provided software using an aqueous buffer model.

Chemotaxis Assays

Optimal concentrations of chemokines (12 nM CCL11, 25 nM CCL24, 100 nM CCL26, and 1 µM platelet-activating factor, PAF) were used to induce cell chemotaxis .[1, 2] CCL11, CCL24, and CCL26 were purchased from BioLegend (San Diego, CA) and PAF (C16) was purchased from Tocris Bioscience (Minneapolis, MN). Inhibitors or controls were placed in both upper and lower chambers of transwell plates with 5 µm pore size membranes (Corning, Kennebunk, ME). For assays used to determine the effect of R321 on the chemotaxis of human peripheral blood eosinophils toward PAF, a PAF receptor inhibitor WEB 2086 was purchased from Tocris Bioscience (Minneapolis, MN) and used at a concentration of 100 µM as a positive control. A total of $1x10^5$ cells were

placed in each well and following 4h of migration cells were counted using flow cytometry (Beckman Quanta SC, Beckman Coulter, Indianapolis, IN).

CCL11-induced secretion of ECP

Purified human peripheral blood eosinophils were resuspended in PBS + 0.1% BSA to a final concentration of 1x 10^6 cells/mL and 100 µL were aliquoted per well. Cells were pretreated for 30 min with 1 µM R321, R323, or vehicle, and stimulated with 12 nM CCL11 for 3h. Following stimulation, cells were centrifuged (1500 rpm, 10 min) and supernatants were collected for further analysis. ECP detection in supernatants was performed using a commercial ELISA kit (MesaCup ECP test, MBL, Woburn, MA).

Detection of ERK 1/2 and AKT

AML14.3D10-CCR3 cells were serum starved for 4h, resuspended in RPMI 1640 + 0.1% BSA to a density of 1x10^7 cells/mL, and then pretreated with either vehicle control (PBS + 1% DMSO) or 10 µM inhibitors (R321, R323, SB238437, or UCB35625) for 30 min at 37℃ and 5% CO_2. Cell aliquots were taken before stimulation and 2.5, 5, 10, 15, and 30 min after stimulation with 100 nM CCL11 and washed in ice cold PBS. Cell pellets were lysed in RIPA lysis buffer (Santa Cruz Biotechnology, Santa Cruz, CA) containing 1mM PMSF, 1mM Na-orthovanadate, 30 mM NaF, and protease inhibitor cocktail tablet (Roche, Indianapolis, IN). Cell lysate proteins were separated on 12% (w/v) SDS-PAGE gels (15µg/ lane) and transferred to PVDF membranes at 20V for 40 min. Membranes were blocked with 5% BSA for 2h at RT, and incubated overnight at +4℃ with rabbit anti-phospho-ERK 1/2 antibodies or rabbit anti-phospho-AKT

antibodies (Cell Signaling Technology, Danvers, MA). The next day, membranes were extensively washed and incubated for 1h at RT with secondary goat anti-rabbit IgG-HRP antibodies (Santa Cruz Biotechnology, Dallas, TX). Western blots were visualized using SuperSignal West Dura Extended Duration Substrate (Thermo Fisher Scientific, Waltham, MA). For loading controls, membranes were stripped for 15 min in mild stripping buffer (1.5% glycine, 0.1% SDS, 1% Tween-20, pH 2.2) and reprobed with rabbit anti-ERK 1/2 antibodies or rabbit anti-AKT antibodies (Cell Signaling Technology, Danvers, MA). Three independent experiments were performed.

Gαi activation

GTP-bound Gαi was detected using a commercial Gαi assay kit (Abcam, Cambridge, MA) with modifications. Briefly, AML14.3D10-CCR3 cells were serum-starved for 16h before being pretreated with 200 ng/ml pertussis toxin for 2h, 10 μM R321 for 30 min, or with vehicle control. Pretreated cells were then stimulated with 8 nM CCL11 or medium for 1 min. The reaction was stopped by adding and washing once in ice cold PBS. Ten (10) million cells were used for each condition. Washed cells were lysed with 1x lysis buffer following manufacturer instructions. For pull-down of active Gαi, mouse anti-GTP bound Gαi antibody was conjugated to Dynabeads Protein G (Life Technologies, Carlsbad, CA) for 15 min at RT. Conjugated beads were washed 3 times with TBST and incubated with cell lysates for 20min at RT. After washing with TBST, bound proteins were eluted by boiling the beads in 2x SDS sample buffer for 5 min. Eluates were resolved by SDS-PAGE and immunoblotted using a polyclonal rabbit anti-total Gαi antibody (Cell Signaling Technology, Danvers, MA).

CCR3 degradation

AML14.3D10-CCR3 cells were resuspended in RPMI1640 + 0.1% BSA. Aliquots of $1x10^6$ cells were pretreated with 10 µM cycloheximide for 1h at 37℃. Some cells were concurrently pretreated with 10 µM R321 for 30 min. Pretreated cells were stimulated with 8 nM CCL11/eotaxin-1 or CCL5/RANTES for 3h to induce receptor degradation. Cells were lysed in RIPA buffer and immunoblotted for CCR3 using a polyclonal rabbit anti-CCR3 antibody (Abcam, Cambridge, MA) followed by goat anti-rabbit IgG-HRP secondary antibody (Santa Cruz Biotechnology, Santa Cruz, CA).

Immunofluorescence and Confocal Microscopy

AML14.3D10-CCR3 cells were serum starved for 4h and then resuspended in RPMI 1640 + 0.1% BSA to a density of $1x10^6$ cells/mL. Cells were pretreated with 10 µM inhibitors (R321, SB238437 or UCB35625) or R323 or vehicle controls for 30 min at 37℃ and then stimulated with 100 nM CCL11. Aliquot s were taken before stimulation and 30 min after chemokine addition. Cytospin preparations were made by centrifugation of the treated cells at 300 rpm (10.16x g) for 5 min onto glass slides in a cytocentrifuge (Cytospin 2, Shandon, Pittsburgh, PA). Cells were fixed in ice cold methanol for 15 min at -20℃ and washed 3 times in 0.1% Triton X-100 in PBS before blocking in 10% normal goat serum in PBS for 2h at RT. The slides were incubated overnight at +4℃ with primary antibodies diluted i n 0.1% normal goat serum in PBS. CCR3 was detected with 5 µg/mL mouse anti-human CCR3 antibody (Biolegend, San Diego, CA) and β-arrestin 2 with rabbit monoclonal anti-human β-arrestin 2 antibody (Cell Signalling Technology, Danvers, MA). After extensive washing in 0.1% Tween-

20, samples were incubated with appropriate AlexaFluor®488- or AlexaFluor®568-conjugated anti-mouse and anti-rabbit secondary antibodies (Cell Signaling Technology, Danvers, MA) used at 1:500 dilution for 1h at RT. After washing, coverslips were mounted on the glass slides with SlowFade Gold antifade reagent with DAPI (Invitrogen, Carlsbad, CA). Images were collected with a Zeiss LSM 700 laser scanning confocal microscope and 100x/1.45 oil immersion objective using Zen software (Carl Zeiss AG, Oberkochen, Germany) and further processed with Photoshop CS5 (Adobe, San Jose, CA). Quantitative colocalization analysis was performed by selecting single cells as regions of interest (n=50 per treatment group) and calculating mean colocalization coefficients by Pearson's correlation method. Data is presented as mean ± SEM. Statistical analysis was performed using GraphPad Prism software (GraphPad, San Diego, CA) by two-way analysis of variance (ANOVA), followed by Tukey *post hoc* analysis.

Cell surface staining and gating strategy for mouse blood eosinophils

Mouse blood (900 µL) was collected by cardiac puncture into EDTA-coated tubes and red blood cell lysis was performed via hypotonic shock with H_2O. White blood cells were washed with PBS and resuspended to 1x 10^6 cells/100 µL of flow cytometry buffer (PBS + 0.1% BSA). Inhibition of non-specific binding to Fc receptors was performed using a rat anti-mouse CD16/CD32 antibody for 5 min at room temperature (BD Biosciences, San Jose, CA). Cells were subsequently stained for 30 min at RT in the dark with the following antibodies: rat anti-mouse CCR3 fluorescein-conjugated antibody (R&D Systems, Minneapolis, MN), PE-conjugated rat anti-mouse Siglec-F antibody (BD

Biosciences, San Jose, CA), and rat anti-mouse PerCP-Cyanine 5.5 Ly-6G (Gr1) antibody (Thermo Fisher Scientific, Waltham, MA). Cells were washed 3x in PBS, resuspended in 2% paraformaldehyde and analyzed immediately on a Quanta SC flow cytometer (Beckman Coulter, Indianapolis, IN). Eosinophils were gated from live cells as SSC^{hi}, Siglec F–CCR3 double positive, $Gr1^{Lo\text{-}neg}$. Results were analyzed using FlowJo software (FlowJo LLC, Ashland, OR).

Bronchoalveolar lavage (BAL)

One day after the last DRA allergen or sham PBS challenge, mice were euthanized and BAL cells were collected by lavage with 2 mL of cold PBS injected into the trachea via a catheter. Total cell counts were performed using a Countess automated cell counter (Thermo Fisher Scientific, Waltham, MA). For differential BAL cell counts, cytospin preparations were stained with Wright-Giemsa stain (Sigma- Aldrich, St. Louis, MO). Cells were classified as macrophages, lymphocytes, neutrophils, and eosinophils by standard morphology and staining. A minimum of 200 cells were counted per slide.

Determination of airway responsiveness to methacholine

Twenty-four hours after the last intranasal challenge, mice were anesthetized and attached to the FlexiVent rodent ventilator/pulmonary mechanics analyzer (Scireq, Montreal, Canada). Baseline respiratory parameters were measured as previously described.[3] Airway reactivity was assessed by measuring response to increasing doses (0, 5, 10, 20, and 40 µg) of methacholine (Sigma, St Louis, MO) administered intravenously via the jugular vein.

Reductive Methylation of Membrane Preparations.

ChemiSCREEN Chem-1 membrane preparations for recombinant human CCR3 (HTS008M) and negative control (HTS000MC1) CCR3-null membranes were purchased from EMD Millipore. Membrane preparation storage buffer contained 50 mM Tris pH 7.4, 10% glycerol and 1% BSA. Glycerol and BSA are important components for the stability and integrity of the membranes, however BSA and Tris interfere with the reductive methylation reaction. Therefore, ^{13}C formaldehyde (catalog # 489417, Aldrich) and borane–ammonia complex (Catalog #682098, Aldrich) were used in excess to ensure labeling of all possible components of the membranes. Upon quenching the reaction with excess Tris-HCl buffer, membrane fractions were separated by ultracentrifugation at 4℃ and the membrane pellets were resuspended in PBS containing 10% glycerol and 1% unlabeled BSA [4]. The latter step was repeated to remove residual labeled components. Reductive methylation of the membrane preparations was performed as described previously [5, 6]. In brief, 20 µl of 1 M borane–ammonia complex (Catalog #682098, Aldrich) and 40 µl of 1 M ^{13}C formaldehyde (Catalog #489417, Aldrich) were added to 1 ml of membrane preparation. This mixture was incubated with stirring for 2 h at 4℃. The addition of borane–ammonia and formaldehyde was repeated, and the mixture was incubated with stirring for 2 more hours. The final 10 µl 1 M borane – ammonia complex was then added and the mixture was incubated at 4℃ overnight with stirring. The reaction was then stopped by adding 110 µl of 2 M Tris·HCl (pH 7.6). Thereafter, the membrane preparations were separated by ultracentrifugation at 4℃ and resuspended in PBS containing 10% glycerol and 1% unlabeled BSA to be used for NMR experiments.

Heteronuclear Single Quantum Coherence (HSQC) NMR

Final samples (200 µl) contained 50% membrane preparation, 10% D_2O (Catalog #151882, Aldrich), 2% DMSO-d_6 (Catalog #156914, Aldrich). CCL11 (eotaxin) was added at a final concentration of 1 µM. The R321 peptide was added at final concentrations of 0.05, 0.4, 2.0, and 10.0 µM. Peptide stocks were prepared in DMSO-d_6 and then diluted in PBS, left overnight and centrifuged before addition to the membrane preparation. Samples were loaded into 3 mm NMR tubes (part # S-3-600-7, Norell). ^{1}H-^{13}C HSQC NMR experiments were carried out on a 900-MHz Bruker Avance Spectrometer equipped with a cryogenic probe. Spectral widths in ω1 and ω2 were 8389.262 Hz and 3519.359 Hz, respectively, the transmitter offsets were positioned at 4.7 p.p.m for the ^{1}H dimension and 40 p.p.m. in the ^{13}C dimension. ^{13}C decoupling was performed with a GARP sequence. 256 complex points with 168 scans per FID were recorded, to ensure a 20.9-Hz resolution per point at 900 MHz before zero filling. The relaxation delay was set to 1.5 s and 32 steady-state scans preceded data acquisition. Total collection time was 20 hours. Data were processed and analyzed using the NMRPipe/NMRDraw software [7]. For dissociation constant (K_d) determination, the data were analyzed using Graph Pad Prism 5 non-linear regression saturation single binding site equation. Mean values and standard deviations were calculated based on different fitting approaches (regular fit, robust fit, and automatic outlier).

REFERENCES

1. Provost V, Larose M-C, Langlois A, Rola-Pleszczynski M, Flamand N, Laviolette M. CCL26/eotaxin-3 is more effective to induce the migration of eosinophils of asthmatics than CCL11/eotaxin-1 and CCL24/eotaxin-2. Journal of Leukocyte Biology 2013; 94:213-22.
2. Miyagawa H, Nabe M, Hopp RJ, Okada C, Bewtra AK, G. T. The effect of WEB 2086 on PAF-induced eosinophil chemotaxis and LTC4 production from eosinophils. Agents and actions 1992; 37:39-43.
3. Pinto LH, Eaton E, Chen B, Fleisher J, Shuste D, McCauley R, et al. Gene-environment interactions in a mutant mouse kindred with native airway constrictor hyperresponsiveness. Mammalian Genome 2008; 19:02-14.
4. Holden P, Horton WA. Crude subcellular fractionation of cultured mammalian cell lines. BMC Res Notes 2009; 2:243.
5. Abraham SJ, Kobayashi T, Solaro RJ, Gaponenko V. Differences in lysine pKa values may be used to improve NMR signal dispersion in reductively methylated proteins. J Biomol NMR 2009; 43:239-46.
6. Tripathi A, Vana PG, Chavan TS, Brueggemann LI, Byron KL, Tarasova NI, et al. Heteromerization of chemokine (C-X-C motif) receptor 4 with alpha1A/B-adrenergic receptors controls alpha1-adrenergic receptor function. Proc Natl Acad Sci U S A 2015; 112:E1659-68.
7. Delaglio F, Grzesiek S, Vuister GW, Zhu G, Pfeifer J, Bax A. NMRPipe: a multidimensional spectral processing system based on UNIX pipes. J Biomol NMR 1995; 6:277-93.

FIGURE LEGENDS

Figure S1. R321 does not inhibit platelet-activating factor (PAF)-mediated chemotaxis of human blood eosinophils. Cells treated with 1μM R321, R323, UCB35625, or SB328437 did not exhibit statistically significant reduction of chemotaxis to 1μM PAF. In contrast, the specific PAF receptor inhibitor WEB 2086 achieved 83.18 ± 2.56% inhibition of PAF-mediated chemotaxis in blood eosinophils. Results are shown as percentage of vehicle chemotaxis and represent mean ± SEM from an experiment performed in triplicate. Compared to vehicle: $^{****}p < 0.0001$.

Figure S2. R321 does not induce or promote degranulation with secretion of ECP in human blood eosinophils. CCL11 (12 nM) induces degranulation with secretion of ECP. R321 (1μM) alone does not induce a statistically significant increase in ECP secretion. Cells concurrently treated with CCL11 (12 nM) and 1μM R321, or R323, did not exhibit statistically significant increases in ECP secretion as compared to CCL11-vehicle treated cells. ^{ns}not significant, $^{*}p < 0.05$.

Figure S3. Representative confocal microscopy images of control cells. The first two panels from the top show AML14.3D10-CCR3 cells stained without primary antibodies or with isotype control of primary antibodies. The bottom panel is included as a positive control and represents AML14.3D10-CCR3 cells stained for CCR3 and β-arrestin 2 after 30 min of stimulation with 100nM CCL11.

Figure S4. R321 promotes CCR3 internalization in AML14.3D10-CCR3 cells over a prolonged incubation period. Cells were cultured with vehicle, inhibitors (1µM), and/ or 12 nM CCL11 for a period of 72h. At 24h intervals cells were assessed for surface expression of CCR3 by staining with PE-conjugated anti-CCR3 antibody and measuring median fluorescence via flow cytometry. Results are shown as surface expression of CCR3 as percentage of vehicle expression and represent mean ± SEM from an experiment performed in triplicate. Compared to vehicle: ^{ns} not significant, $*p < 0.05$, $****p < 0.0001$.

Figure S5. Triple allergen (DRA) acute asthma model protocol in Balb/c mice. Allergen sensitization/challenge protocol is indicated. Mice were challenged in their airways with DRA allergen or PBS control on days 12-14 via intranasal insufflation (black arrows). Treatment with CCR3 R321 peptide nanoparticles, scrambled R323 control peptide or vehicle was given: **(A) Prophylactically** starting on day 11 before the i.n. allergen challenges on days 11–14 (**blue arrows**) or **(B) Therapeutically** starting on day 14, after the last i.n. allergen challenge (**red arrows**).

Figure S6. R321 and R323 treatment does not lead to significant changes in total numbers of macrophages, neutrophils, or lymphocytes in lung airways. Total macrophage, neutrophil, and lymphocyte cell numbers in the BAL fluid of triple-allergen (DRA) challenged mice remain unchanged at even the highest doses of R321 and R323. R323 was administered at 12 mg/kg. The mean ± SEM are shown for 6-7 mice/treatment group from 3 independent experiments.

Figure S7. R321 binds CCR3+ membrane preparations in the absence of CCL11. (**A**) Overall strategy to label CCR3 membrane preparations using ^{13}C labeled formaldehyde and borane-ammonia complex. (**B**) ^{13}C HSQC spectra of ^{13}C-reductively methylated CCR3 membrane preparations with signal designations indicated. (**C**) Determination of the dissociation rate constant (K_d) for R321 (0.05-10 µM) binding to CCR3 membrane preparations in the absence of CCL11 shows that R321 affects the intensities of signal 1 and signal 2 with K_d values of 1.604 ± 0.010 µM and 0.014 ± 0.001 µM, respectively, while having no effect on signals 3 and 4 that are present on CCR3 null membranes.

Figure S8. Evaluation of CCL11 binding to CCR3 null membrane preparations. ^{13}C HSQC spectra of ^{13}C-reductively methylated CCR3 null membranes were recorded with 1 µM CCL11. Spectral comparisons between reductively methylated CCR3 null membranes (CCR3-K-di$^{13}CH_3$) (red) and CCR3 null membranes + CCL11 (blue) do not show any signal changes indicative of significant binding. Western blot analysis of membrane preparations from Chem-1 cells overexpressing CCR3 and CCR3 null cells shows the absence of CCR3 expression in the null membranes.

Figure S9. R321 induces concentration-dependent spectral changes in CCR3 membrane preparations. ^{13}C HSQC spectra of ^{13}C-reductively methylated CCR3 membrane preparations were recorded with R321 at 0.05, 0.4, 2.0, 10.0 µM. Spectral comparisons are shown for CCR3 alone (CCR3-K-di$^{13}CH_3$) (**red**) and CCR3 + R321 (**blue**) at (**A**) 0.05 µM, (**B**) 0.4 µM, (**C**) 2.0 µM, (**D**) 10.0 µM, show chemical shift

changes indicative of binding. Black arrows show significant changes in signal line widths and chemical shifts.

Figure S10. Schematic of the CCR3 signaling pathway and proposed R321 mechanism of inhibition. (A) Agonist receptor binding leads to activation of the G-protein dependent signaling cascade resulting in eosinophil chemotaxis, secretion and degranulation. Upon prolonged exposure to agonist, CCR3 is desensitized and internalized via a β-arrestin mediated endocytic pathway. **(B)** R321 nanoparticles dissipate upon contact with the cell membrane, allowing the R321 peptide monomer to displace the CCR3 TM2 helix. R321 binding alters the CCR3 structure in a manner that inhibits G-protein dependent signaling but not β-arrestin-mediated internalization (endocytosis) and degradation of CCR3.

Figure S1

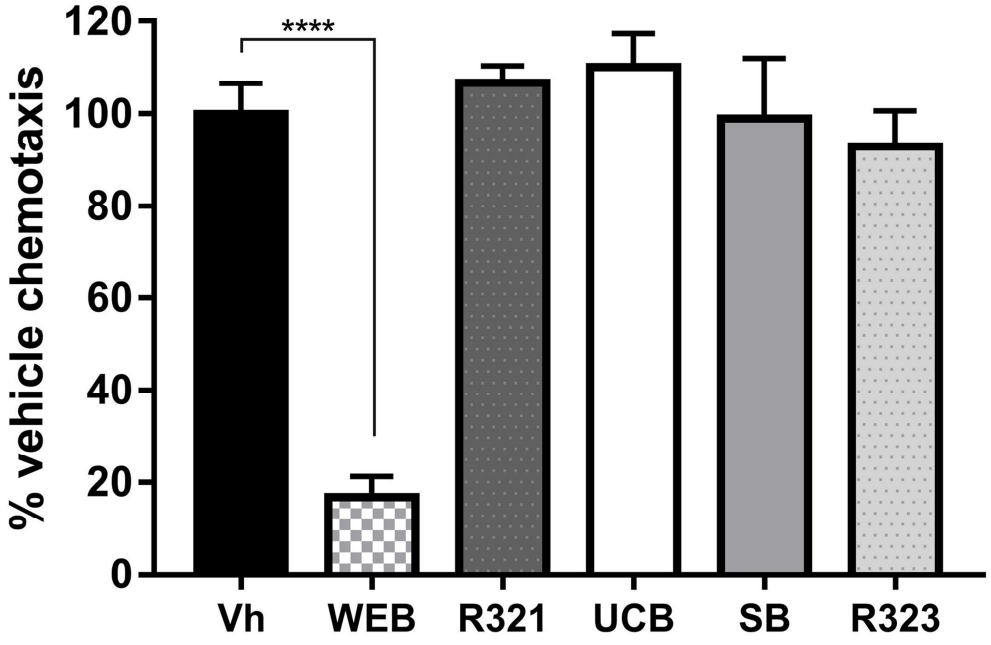
% vehicle chemotaxis
120
100
80
60
40
20
0
****
Vh
WEB
R321
UCB
SB
R323

Figure S2.

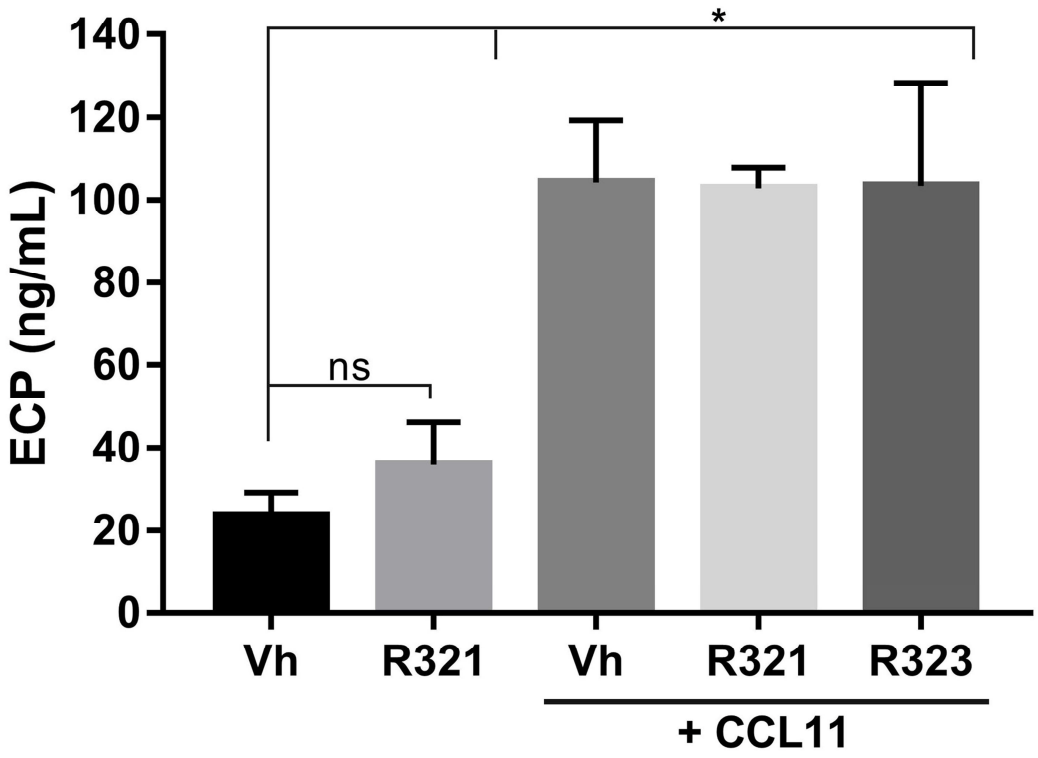

Figure S3

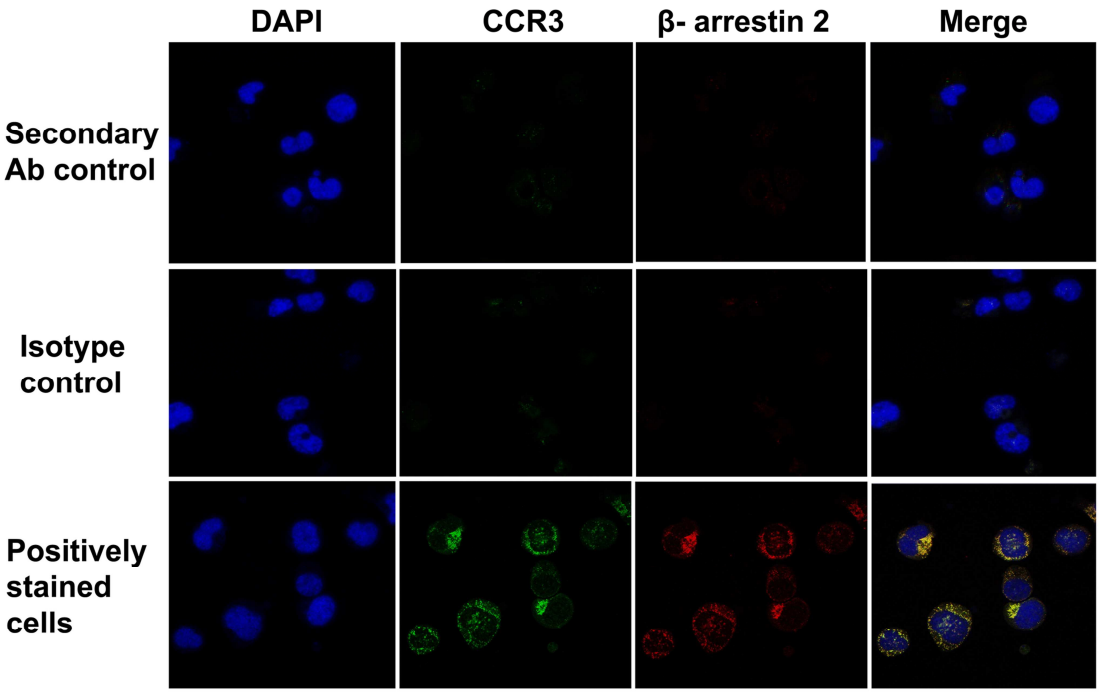
DAPI
CCR3
β- arrestin 2
Merge
Secondary Ab control
Isotype control
Positively stained cells

Figure S4

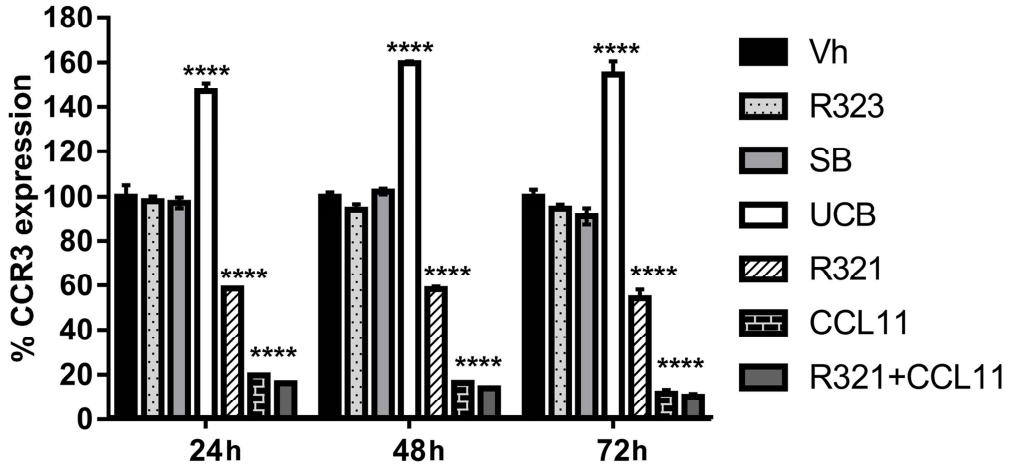
% CCR3 expression
180
160
140
120
100
80
60
40
20
0
****
****
****
****
****
****
24h
48h
72h
Vh
R323
SB
UCB
R321
CCL11
R321+CCL11

Figure S5

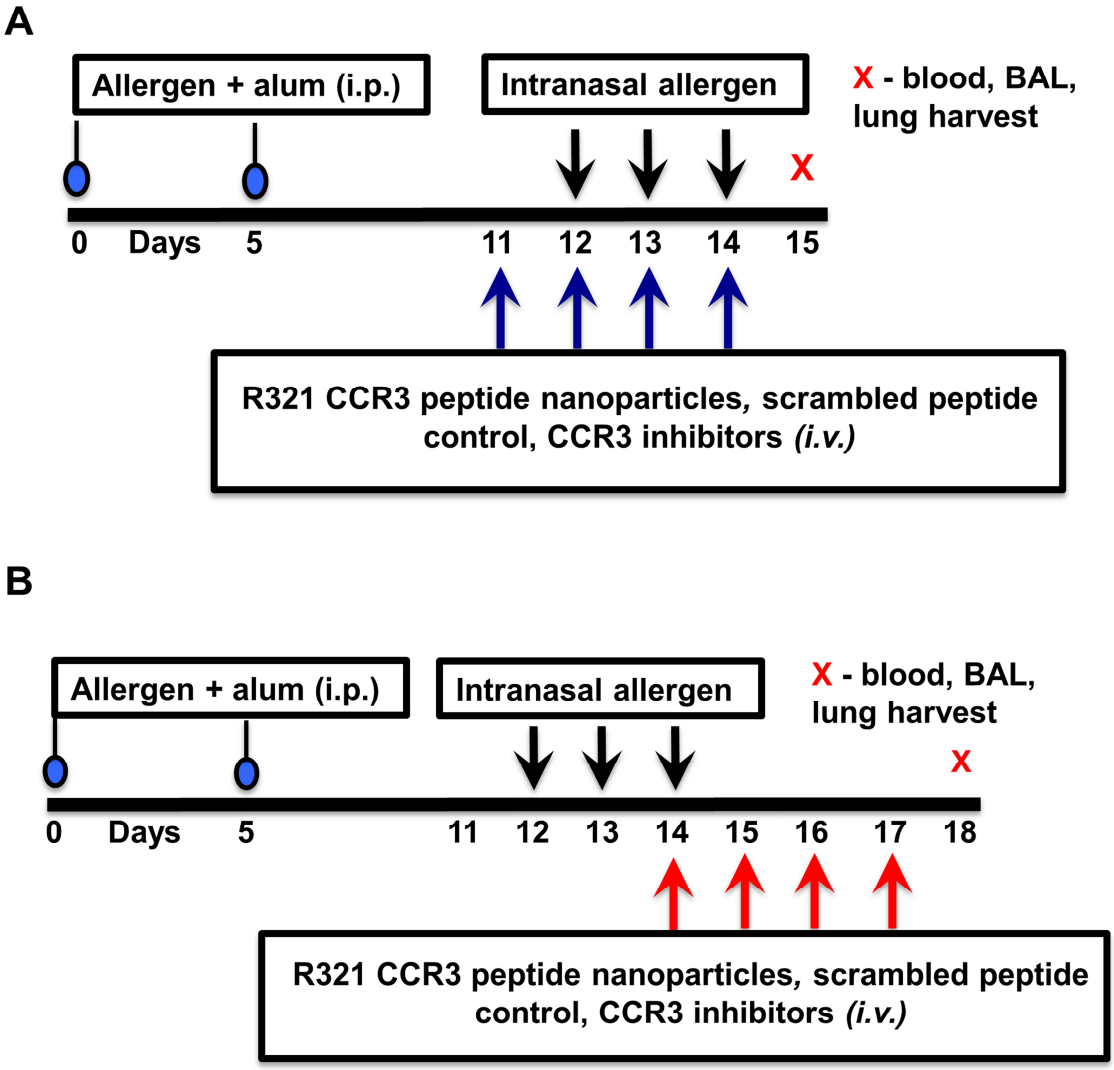
A
Allergen + alum (i.p.)
Intranasal allergen
X - blood, BAL, lung harvest
X
0 Days 5 11 12 13 14 15
R321 CCR3 peptide nanoparticles, scrambled peptide control, CCR3 inhibitors (i.v.)
B
Allergen + alum (i.p.)
Intranasal allergen
X - blood, BAL, lung harvest
X
0 Days 5 11 12 13 14 15 16 17 18
R321 CCR3 peptide nanoparticles, scrambled peptide control, CCR3 inhibitors (i.v.)

Figure S6

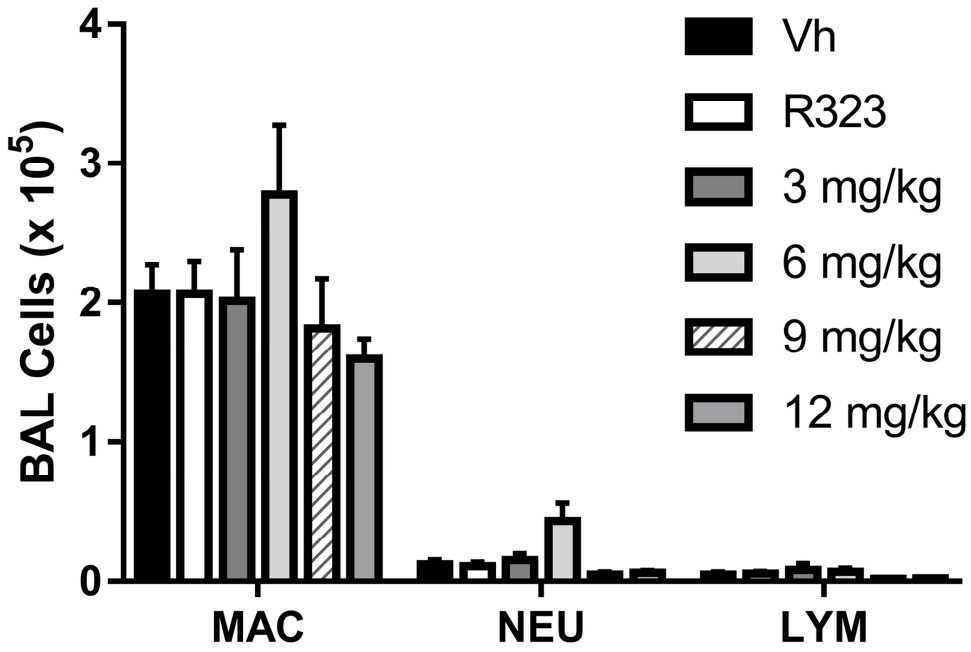
BAL Cells (x 10^5)
4
3
2
1
0
MAC
NEU
LYM
Vh
R323
3 mg/kg
6 mg/kg
9 mg/kg
12 mg/kg

Figure S7

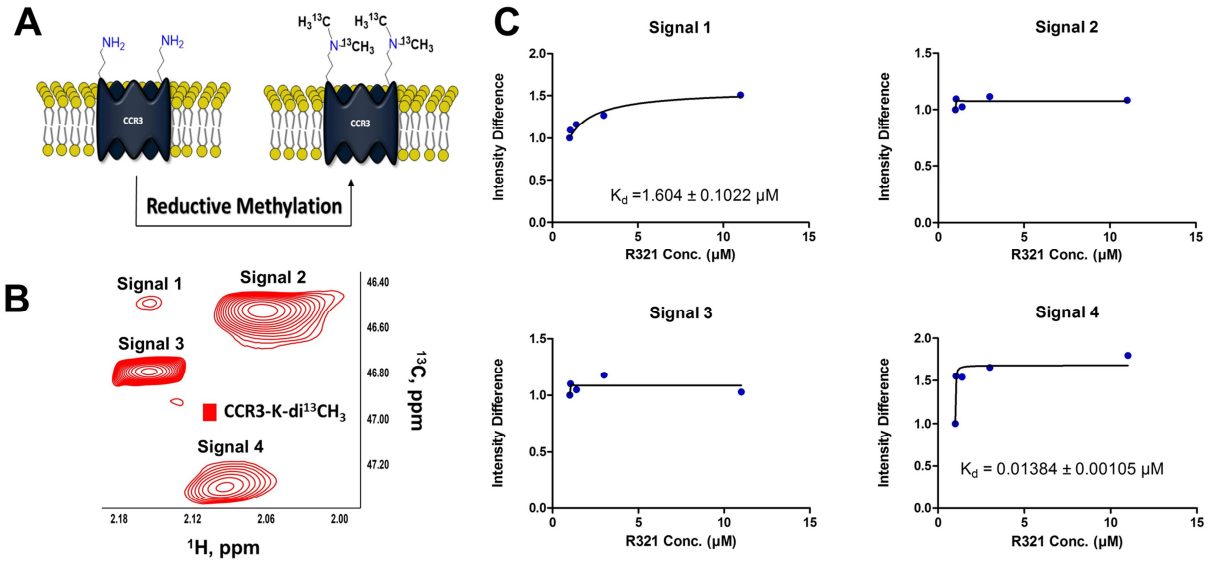
A
NH2
NH2
CCR3
H3 13C
H3 13C
N-13CH3
N-13CH3
CCR3
Reductive Methylation
B
Signal 1
Signal 2
Signal 3
CCR3-K-di13CH3
Signal 4
46.40
46.60
46.80
47.00
47.20
13C, ppm
2.18
2.12
2.06
2.00
1H, ppm
C
Signal 1
Kd =1.604 ± 0.1022 μM
Intensity Difference
R321 Conc. (μM)
Signal 2
Intensity Difference
R321 Conc. (μM)
Signal 3
Intensity Difference
R321 Conc. (μM)
Signal 4
Kd = 0.01384 ± 0.00105 μM
Intensity Difference
R321 Conc. (μM)

Figure S8

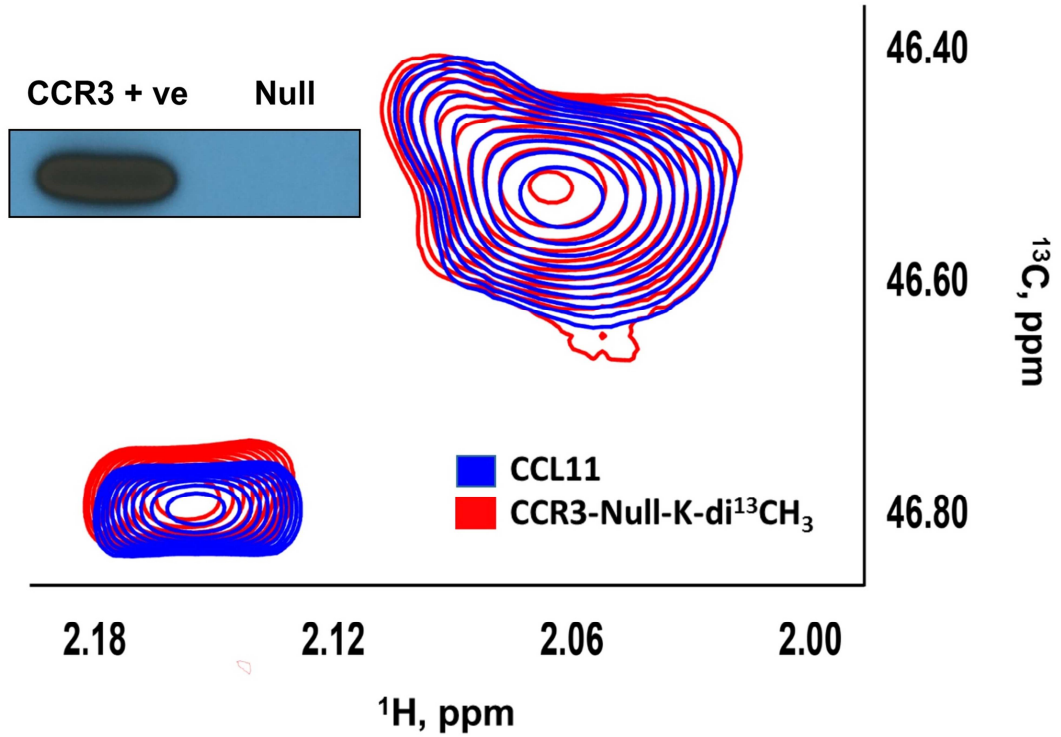
CCR3 + ve
Null
46.40
46.60
46.80
^{13}C, ppm
CCL11
CCR3-Null-K-di^{13}CH$_3$
2.18
2.12
2.06
2.00
^{1}H, ppm

Figure S9

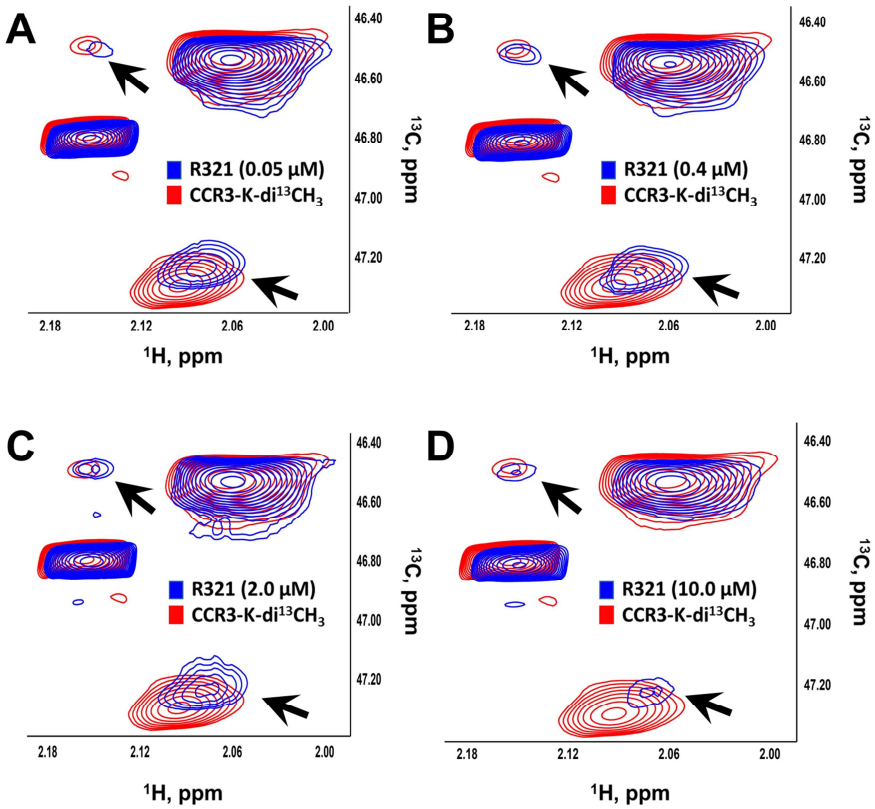
A
B
C
D
R321 (0.05 µM)
R321 (0.4 µM)
R321 (2.0 µM)
R321 (10.0 µM)
CCR3-K-di13CH3
13C, ppm
1H, ppm
46.40
46.60
46.80
47.00
47.20
2.18
2.12
2.06
2.00

Figure S10